Functional Analogues of Cytochrome *c* Oxidase, Myoglobin, and Hemoglobin

James P. Collman,* Roman Boulatov, Christopher J. Sunderland, and Lei Fu

Department of Chemistry, Stanford University, Stanford, California 94305

Received April 22, 2003

Contents

1. Introduction

The majority of modern organisms, including many prokaryotes, are aerobes;[1] that is, they use molecular oxygen as the terminal electron acceptor for energy generation. Although nearly every redox gradient in nature appears to be utilized by one organism or another,[2−4] aerobic metabolism predominates, in large part due to the highly exergonic nature of the four-electron, four-proton ($4e/4H^+$) reduction of O_2 to H_2O (reaction 1). A multicellular aerobe requires an

$$O_2 + 4H^+ + 4e^- \rightleftharpoons 2H_2O$$
$$\Delta E°(\text{pH } 7) = 0.8 \text{ V}; \Delta G° = 80 \text{ kcal/mol} \quad (1)$$

efficient means not only of catalyzing the fast reduction of O_2 to H_2O without generating toxic partially reduced oxygen species, but also of delivering O_2 to, and storing O_2 in, various cells. In humans, O_2 reduction catalysis, dioxygen transport, and storage are performed by cytochrome *c* oxidase (CcO),[5−14] hemoglobin (Hb),[15−18] and myoglobin (Mb),[15,19−21] respectively.

The functional and structural complexity of these components of aerobic metabolism increases from myoglobin to cytochrome *c* oxidase, and correspondingly our understanding of them decreases in the same order. Myoglobin is a monomeric protein containing a single five-coordinate heme whose function is to reversibly form a dioxygen adduct while avoiding irreversible heme autoxidation. Our current understanding of the stereoelectronic requirements for such reactivity derives in large part from studies of synthetic heme−dioxygen complexes.[22] Picket-fence porphyrins (see section 2.2) afforded the first unambiguous implementation of the idea that reversible oxygenation of myoglobin and hemoglobin is possible because the five-coordinate ferrous heme is immobilized in a sterically hindered hydrophobic matrix. Subsequent studies of dioxygen reactivity of superstructured porphyrins have contributed to our understanding of related physiologically important problems, for example, the origin of O_2 vs CO discrimination by Mb and Hb.[23−25] However, despite an enormous amount of biochemical and biomimetic data, we still lack adequate knowledge of such issues as a quantitative correlation between the properties of the O_2-binding pocket (such as polarity and the number and position of hydrogen bonds) and the O_2 affinity of the heme, and the mechanism(s) of the autoxidation of O_2 adducts.[26] Indeed, while numerous face-protected porphyrins bind O_2 reversibly in nonprotic media, few synthetic systems form O_2 adducts that do not undergo rapid autoxidation in an aqueous solution.[27−30]

In contrast to myoglobin, O_2-transporting human hemoglobin is a tetramer,[31,32] which cooperatively binds four O_2 molecules. Whereas our understanding of the basis of cooperativity in hemoglobin is rather sophisticated,[17] the biologically relevant mechanism of homoallosteric O_2 binding is yet to be reproduced outside the protein matrix. Only a few notable attempts have been made. This topic is worth pursuing vigorously because a biologically relevant model of cooperative O_2 binding should reveal the minimum structural requirements for cooperativity and can help better understand the energetics of allosteric control in Hb (e.g., the relative contribution of protein solvation).

10.1021/cr0206059 CCC: $48.50
Published on Web 12/16/2003

James P. Collman was born in 1932 and received B.S. and M.S. degrees from the University of Nebraska in 1954 and 1956, and a Ph.D. from the University of Illinois in 1958 under the supervision of R. C. Fuson. In 1958–1967 he was on the faculty of the University of North Carolina at Chapel Hill; he moved to Stanford in 1967, where he is Daubert Professor of Chemistry. His research interests are very broad, extending across inorganic and organic chemistry, and also include superconductivity. His principal research is directed toward the development of structural and functional analogues of the active sites in heme proteins, particularly cytochrome oxidase. His work has been recognized by many awards; he is a member of the National Academy of Sciences.

Roman Boulatov received his Ph.D. in chemistry from Stanford in 2002, working under the guidance of Prof. James P. Collman on biomimetic studies of cytochrome *c* oxidase, utilization of metalloporphyrins for catalysis of multielectron reductions, and creation of new bonds between transition metals stabilized by porphyrins. Currently, he is a postdoc in the laboratories of Professor George M. Whitesides at Harvard, working on several problems in nanoscience. Boulatov's scientific accolades include the IUPAC Prize for young chemists (2002), a Stanford Graduate Fellowship (1998–2002), and a Presidential Fellowship (Russia, 1994–1996).

Cytochrome *c* oxidase (CcO) contains several redox cofactors in addition to the bimetallic, heme/Cu, catalytic site at which O_2 is reduced. The enzyme utilizes a large fraction of the free energy released in O_2 reduction to translocate protons from the mitochondrial matrix to the intermembrane space, working against the electrochemical proton gradient.[12,13,33,34] In 1995, nearly simultaneous publication of single-crystal X-ray diffraction structures of bovine heart CcO by Yoshikawa[35] and of bacterial CcO by Iwata[36] enormously facilitated both biochemical and biomimetic studies of cytochrome *c* oxidase. Numerous details regarding the O_2 reduction mechanism of, and proton pumping by, CcO have been uncovered, but many important questions remain unanswered.

Christopher Sunderland was born in Luton, England, in 1969. Raised in Australia, he gained a B.Sc. in chemistry from the University of Queensland in 1992. After moving to California, he graduated from U.C. Berkeley in 1998, studying novel gadolinium MRI contrast agents in Prof. Ken Raymond's group. He is now a research associate in Prof. James Collman's group at Stanford University, working on synthetic and reactivity studies of biomimetic models of terminal oxidases.

Lei Fu received his Ph.D. degree from Stanford University in 1997 under the direction of Professor James P. Collman. As a postdoctoral associate, he continued his research with Dr. Collman on biomimetic models of myoglobin and cytochrome *c* oxidase. In 1998, he assumed his current position in analytical and drug discovery/development at Pharmacyclics. Before starting graduate school at Stanford, he was a lecturer and research associate at Fudan University, China, where he earned his B.Sc. and M.Sc. degrees. He also worked as an invited scientist at the Free University of Berlin, Germany.

This review is limited to *functional* synthetic analogues of these three heme proteins: myoglobin, hemoglobin, and cytochrome *c* oxidase. For the purpose of this review, we define functional analogues of myoglobin as synthetic Fe porphyrins whose O_2 adducts are formed reversibly in solution at close to ambient temperature and are stable enough to be studied by conventional spectroscopic techniques ($\tau_{1/2} > 10$ s). Because cooperativity is essential for the biological function of Hb, in this review we consider as functional hemoglobin analogues only those molecules that bind O_2 reversibly and cooperatively. Similarly, since the physiological function of cytochrome *c* oxidase is to catalyze reduction of O_2 to H_2O, we limit our discussion to systems that both reproduce the structural motif of the heme/Cu site and catalyze $4e^-/4H^+$ reduction of O_2 under physiologically relevant conditions. This excludes cofacial diporphyrins,[37,38] which are efficient O_2 reduction catalysts but whose structure is more relevant to the

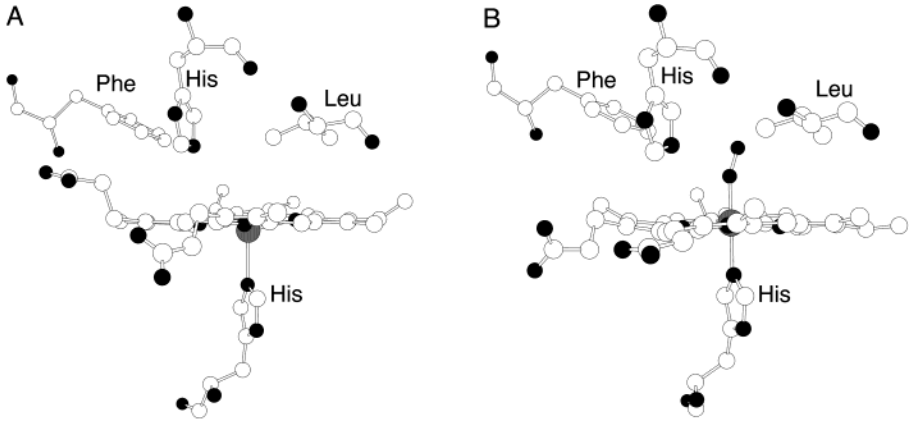

Figure 1. O_2-binding site in (A) human deoxy-Hb[52] and (B) fully oxygenated Hb.[53] Note the in-plane movement of Fe. The distal imidazole is positioned so as to facilitate hydrogen bonding between the $N_\epsilon-H$ moiety (not shown) and O atoms of coordinated dioxygen. White circles are C atoms, Fe is gray, and O and N atoms are black. Generated using Rasmol from PDB files 1A3N and 1HHO.

catalytic site of alternative oxidases.[39] The O_2 reactivity of CcO analogues under stoichiometric, nonprotic conditions, which is a very active area of biomimetic studies of CcO, is described in detail by Karlin in this issue.[40] Modified proteins, heme/oligopeptide assemblies, and related systems based on biomolecules are also excluded from this review but have been summarized elsewhere.[41−43]

The last comprehensive review of synthetic heme−O_2 adducts was published about 10 years ago by Momenteau and Reed,[22] although selected aspects of this area have been reviewed since then.[24,44] Here we avoid duplicating Momenteau and Reed's coverage. In addition to summarizing the results that have been reported after 1994, we review CO binding studies in the context of the possible origin of CO vs O_2 discrimination by globins, cooperative O_2 binding, and synthetic reversible O_2 carriers operating in protic media. These topics either were not covered or were covered only in passing in the 1994 review. Biomimetic studies of cytochrome oxidase have been reviewed more recently;[37,45] here we largely concentrate on the results that have appeared since and have not been reviewed elsewhere.

2. Biomimetic Analogues of Hemoglobin and Myoglobin

2.1. The Proteins

Hemoglobin (Hb) and myoglobin (Mb) are responsible for the transport and storage of O_2, respectively, in many aerobic organisms. The first X-ray crystal structures of Mb and Hb were determined as early as the late 1950s,[46−49] and now atomic-resolution structures of Mb are available in several ligation states.[50,51] Myoglobin contains one heme (iron protoporphyrin IX); hemoglobin consists of four Mb-like subunits each containing a heme. The O_2-binding sites in Hb and Mb are very similar. In its deoxy form (Figure 1), the ferrous ion of the heme is in a five-coordinate high-spin state ($S = 2$), with imidazole serving as the axial ligand on the proximal side. Dioxygen binds at the sixth (distal) vacant coordination site. Binding of O_2 causes an in-plane movement

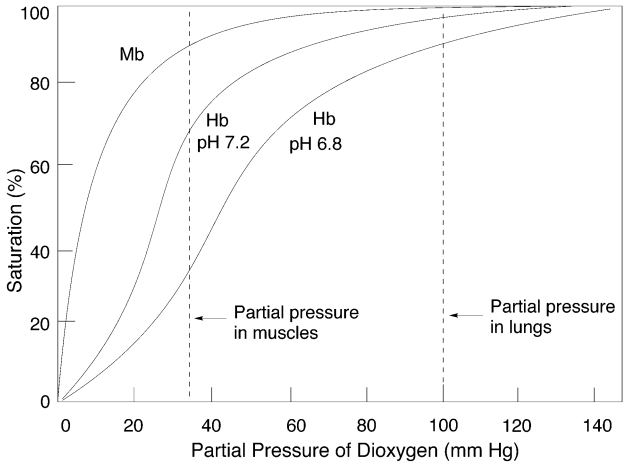

Figure 2. Equilibrium fraction of oxyMb and oxyHb as a function of the O_2 pressure. The O_2 affinity of Hb is subject to both homoallosteric control (i.e., the affinity depends on the O_2 concentration, or partial pressure) and heteroallosteric control (the effect of H^+ is shown as an example).

of the Fe, resulting from shortening of the Fe−N distances, as well as conformational changes within the porphyrin macrocycle and the distal protein residues.

Myoglobin stores O_2 in muscles in order to permit short bursts of aerobic metabolism at rates much greater than those which would be allowed by just circulatory oxygen transport. The latter function is performed by hemoglobin, which adjusts its binding affinity to various conditions required for appropriate uptake and release of O_2 through a series of allosteric interactions. As a result, the O_2 binding affinity of Hb depends on the partial pressure of O_2, as well as pH, Cl^- concentration, etc. In contrast to the simple hyperbolic curve expected for any O_2 binder whose affinity is independent of the O_2 partial pressure (a non-cooperative binder such as Mb), Hb's dependence is sigmoidal (Figure 2). Through this homoallosteric effect,[54] the affinity of Hb for small ligands (such as O_2 or CO for ferroHb and CN^- for metHb) increases with the concentration of the ligand. Such cooperative binding is presently explained by a two-state allosteric mechanism which postulates that Hb exists in two stable conformations (T for "tense" and R for

"relaxed") having different ligand affinities. The trigger mechanism for the T-to-R conversion, at least in ferroHb, is an in-plane movement of the ferrous ion, which converts from the high- to low-spin state upon coordination of the exogenous ligand. This movement is transmitted through conformational changes within the protein matrix to the subunit interface, where it leads to the disruption of salt bridges. The endergonicity of the latter transformation accounts for the lower ligand affinity of the T-state Hb.

Heme ligand affinities are also regulated by polar, hydrophobic, and/or steric interactions between heme-bound exogenous ligands and the distal amino acid residues. The most significant distal effect invoked in the stabilization of O_2 in oxy-Mb and oxy-Hb is a hydrogen-bonding interaction between bound O_2 and the distal histidine (Figure 2). Initially proposed by Pauling,[55] the existence of the H-bond was at first shown by EPR and resonance Raman studies of cobalt-substituted oxyhemoglobin.[56] Subsequent X-ray structure analysis[53,57] and neutron diffraction studies[58] on oxy-Mb and oxy-Hb provided direct evidence for such hydrogen bonding. Appropriately positioned hydrogen bonds can dramatically increase the O_2 affinity: for example, the 10^4-fold higher O_2 affinity of a unique hemoglobin from the bloodworm *Ascaris* relative to human Hb is thought to result from multiple H-bonds between coordinated dioxygen and distal Tyr and Glu residues.[59]

In addition to O_2, CO is a biologically significant ligand for Mb and Hb. The in vivo degradation of heme generates one molecule of CO per heme catabolized, resulting in a partial pressure of CO on the order of 1×10^{-3} Torr at the cellular level.[60] Because CO has a high affinity to ferrohemes, it is a potentially powerful endogenous inhibitor of certain hemoproteins. Outside the protein matrix, imidazole-ligated heme has a CO affinity much greater than that of Mb or Hb, indicating that the globin disfavors CO binding.[61] It is generally accepted now that distal amino acids stabilize the dioxygen adduct while destabilizing the CO analogue. The atomic mechanism of the globin's discrimination against CO has been extensively studied both biochemically and biomimetically, but it remains one of the more controversial issues in the biochemistry of Mb and Hb.

The ratio of the half-saturation pressures of O_2 and CO ($p_{1/2}{}^{O_2}/p_{1/2}{}^{CO}$), referred to as the *M* value, is a useful measure of a complex's susceptibility to CO inhibition. Hb and Mb are clearly designed by nature to transport and store O_2 in the presence of the endogenous poison, CO. Typical *M* values for Mb and Hb are $\sim 10^2$, whereas the intrinsic affinity of the imidazole-ligated heme for CO is $>10^4$ times than that for O_2. Steric, electrostatic, and H-bonding properties of the distal pocket appear to contribute to discrimination of CO vs O_2, which have different properties as ligands. Whereas CO prefers to bind normal to the heme plane, the O_2 adduct is intrinsically bent (Figure 1B). Likewise, substantial localization of the negative charge at the distal O of oxyheme (which is often viewed as a ferriheme−superoxide adduct) contrasts with little charge separation in the heme−CO adduct. Distal groups have been shown to affect Mb's *M* values.[62] The consensus opinion in the field appears to be that spectroscopic data collected on Mb−CO in the past 25 years indicate a slightly bent Fe−C−O unit (5−10°), which is also tilted by 5−10° from the axis normal to the average 24-atom plane of the porphyrin.[25] Indeed, even in synthetic hemes with sterically-induced very low affinity to CO, no significant distortion of the Fe−C−O unit is observed.[24] Analysis of the kinetic and equilibrium data for various Mb mutants suggests that the steric strain, accommodated by a distortion of the Fe−C−O unit and of the globin, accounts for <20% of the difference in CO affinities of the heme vs Mb. It was argued that electrostatic and H-bonding effects are mainly responsible for CO vs O_2 discrimination by Mb and Hb.[25,63] However, the quantitative contributions of each of these factors remain a contentious issue. For example, Jameson analyzed the O_2 and CO binding affinities of a series of Mb mutants and concluded that factors stabilizing O_2 binding and destabilizing CO binding correlate only weakly.[64]

Confusion about the stereoelectronic effects of the distal environment on the affinities of gaseous molecules to globins has been compounded by a tacit assumption by many workers in the field that kinetically determined equilibrium constants (k_+/k_-) for CO and O_2 binding are equivalent to those measured thermodynamically. However, thermodynamically and kinetically derived equilibrium constants may differ by as much as a factor of 5.[65] This happens when O_2 diffusion through the protein matrix to the O_2-binding site has activation barrier(s) comparable to the activation barriers of steps involved in the Fe−O bond homolysis/formation. The latter reaction is traditionally studied in kinetic photolysis experiments. As a result, the kinetic experiments quantify a process that is but one step of a more complex reaction studied in equilibrium measurements. The difference between the kinetically and thermodynamically determined equilibrium constants is expected to be less significant, if at all, in small-molecule Mb analogues, wherein Fe is generally easily accessible.

In addition to preventing irreversible aerobic oxidation of ferroheme through the intermediacy of peroxo-bridged hemes, the globins stabilize oxyheme against heterolytic cleavage of the Fe−O bond, which results in the release of superoxide (autoxidation). Prevention of such a process is important both because superoxide is toxic and because the resulting ferriheme cannot serve as an oxygen carrier. Even though autoxidation of human Mb and Hb under physiological conditions is relatively slow (the apparent rate constant <0.01 h^{-1}, $\tau_{1/2} > 60$ h), about 1−2% of all Hb in a human is in the ferric (met) form at any given time.[26] The autoxidation is slowest at pH 7.5−9 (depending on the protein) and is accelerated by orders of magnitude both in more and in less acidic solutions; the rate also depends on the partial pressure of O_2. The mechanism of autoxidation remains uncertain. Neither outer-sphere electron transfer nor spontaneous dissociation of O_2^- from

oxyheme is thought to operate. The so-called "acid-catalyzed two-state model" postulates that autoxidation proceeds via either spontaneous dissociation or an S_N2 displacement of HO_2 from protonated oxyheme. This process is thought to be accelerated by a factor of $>10^6$ as a result of directed H^+ transfer from a protonated amino acid residue to the distal O atom of the oxyheme. The distal imidazole that forms a H-bond to the coordinated dioxygen was proposed to be the residue that facilitates H^+ transfer from solvent to oxyheme by a "proton relay mechanism".[26] This hypothesis is supported by the absence of a pH dependence for the autoxidation rate at pH < 6 of myoglobins lacking the distal imidazole[26] and also by a dramatic increase in autoxidation rates of Mb mutants where the native distal histidine is substituted by an amino acid that places a more acidic residue in the close proximity of the bound dioxygen.[21] However, replacement of the imidazole with a hydrophobic residue also accelerates autoxidation (by a factor of 100−800). On the basis of this observation, the importance of the proton-relay mechanism in globin autoxidation was questioned.[21] S_N2 displacement of O_2^- from oxyheme by a nucleophile was also proposed to explain the accelerating effects of OH^-, N_3^-, CN^-, OCN^-, F^-, SCN^-, etc. on autoxidation at neutral pH.[26]

How the globin stabilizes oxyheme against O_2^--releasing autoxidation remains unclear. Denaturated oxyMb autooxidizes $>10^3$ faster than the native form.[26] It was therefore suggested that the protein matrix limits the access of charged species (such as H^+ or a nucleophile) to the oxyheme moiety. However, protecting effects of the H-bond and of the distal imidazole as an H^+ scavenger were also proposed as dominant factors.[21]

2.2. Synthetic Analogues of Mb

The basic requirements for reversible O_2 binding in nonprotic media—five-coordinate Fe porphyrin with bulky peripheral substituents, face differentiation and axial monoligation, epitomized by the picket-fence porphyrin **1a** (Figure 3)—are now well established, and the chemical implementation of these principles have been extensively reviewed, particularly by Momenteau and Reed in 1994.[22] In the past 10 years since their review appeared, several new classes of myoglobin models have been reported, such as twin-coronet and dendritic porphyrins, and additional, more elaborate members of the "classical" types, such as picket-fence and capped porphyrins, have been synthesized and studied. These novel porphyrin ligands increasingly often carry an imidazole or a pyridine moiety linked to the porphyrin in a way to favor intramolecular proximal ligation and to prevent intermolecular binding. This design eliminates the need to use a large excess of exogenous nitrogenous heterocycle in gas binding studies and hence the associated complications. Novel synthetic methodologies that have been applied to synthesis of Mb analogues include the "congruent multiple Michael addition"[66] and more efficient face differentiation and atropomer enrichment techniques (see below).[67] Since 1994, several new single-crystal X-ray diffraction structures of Mb models have appeared,[24,68−70] further facilitating our understanding of the structure/reactivity relationships.

Several directions in biomimetic studies of Mb and Hb currently have special relevance and are expected to further our understanding of the biochemistry and biophysics of biological heme-based oxygen carriers. These include (i) the steroelectronic origin of CO vs O_2 discrimination; (ii) the role of the distal environment in modulating the O_2 affinity of the heme; (iii) the mechanism of H^+-coupled autoxidation of oxyheme (which requires development of synthetic porphyrins capable of reversible O_2 binding in protic media), and (iv) reproducing the "trigger" mechanism of cooperative oxygenation of Hb. The current state-of-the-knowledge of these topics is covered in the following sections.

2.2.1. The Molecular Origin of CO vs O_2 Discrimination by Mb and Hb

In 1976, Collman, Brauman, and co-workers noted that different steric requirements of CO and O_2 as ligands can form a molecular basis for discrimination against binding of CO vs O_2 to Fe porphyrins.[87] Because CO coordination requires a linear M−C−O geometry, whereas the O_2 adduct is bent, central steric hindrance (i.e., that directly over the porphyrin ring) should have more pronounced effects on CO rather than O_2 affinities, whereas peripheral (side-on) interactions should influence O_2 binding more strongly. This simple hypothesis has proven to be a remarkably successful paradigm for design of synthetic porphyrins whose *M* values vary over 7 orders of magnitude, from $> \sim 10^5$ for porphyrins **2c**,[73] **4**,[75] **6a**,[78] and **11a**[82] (Figures 3 and 4 and Table 1) to <0.003 in **13b**.[66] Indeed, with the exception of a recent dendritic Mb model **17**, synthetic Fe porphyrins with low *M* values (>200) were designed on the basis of this paradigm.

With respect to CO binding (Table 1), biomimetic Mb analogues appear to form two broad thermodynamically homogeneous groups based on statistical analysis of the respective linear free-energy relationship (Figure 6). It is apparent from Figure 6A that the groups differ notably in the reactant-like character of the respective transition-states. The stereoelectronic characteristics of each group are, however, not clear at present, in part because only porphyrins with relatively low CO affinity ($p_{1/2} > 10^{-3}$ Torr) could be reliably assigned to each of the groups, due to the apparent overlap between the two LFERs. No statistically meaningful trends with respect to the nature of the proximal ligand (mim, dmim, or dcim), the type of the porphyrin (TPP-type or pyrrole-substituted), or the type of the superstructure were observed. This suggests that these types of stereoelectronic perturbations are thermodynamically equivalent with respect to CO binding. While application of LFER to sufficiently limited sets of porphyrins (e.g., **7**(mim) or **7**(dmim)) suppresses scatter enough to identify a larger number of smaller groups,[22,80,88] global analysis, which is more informative in the

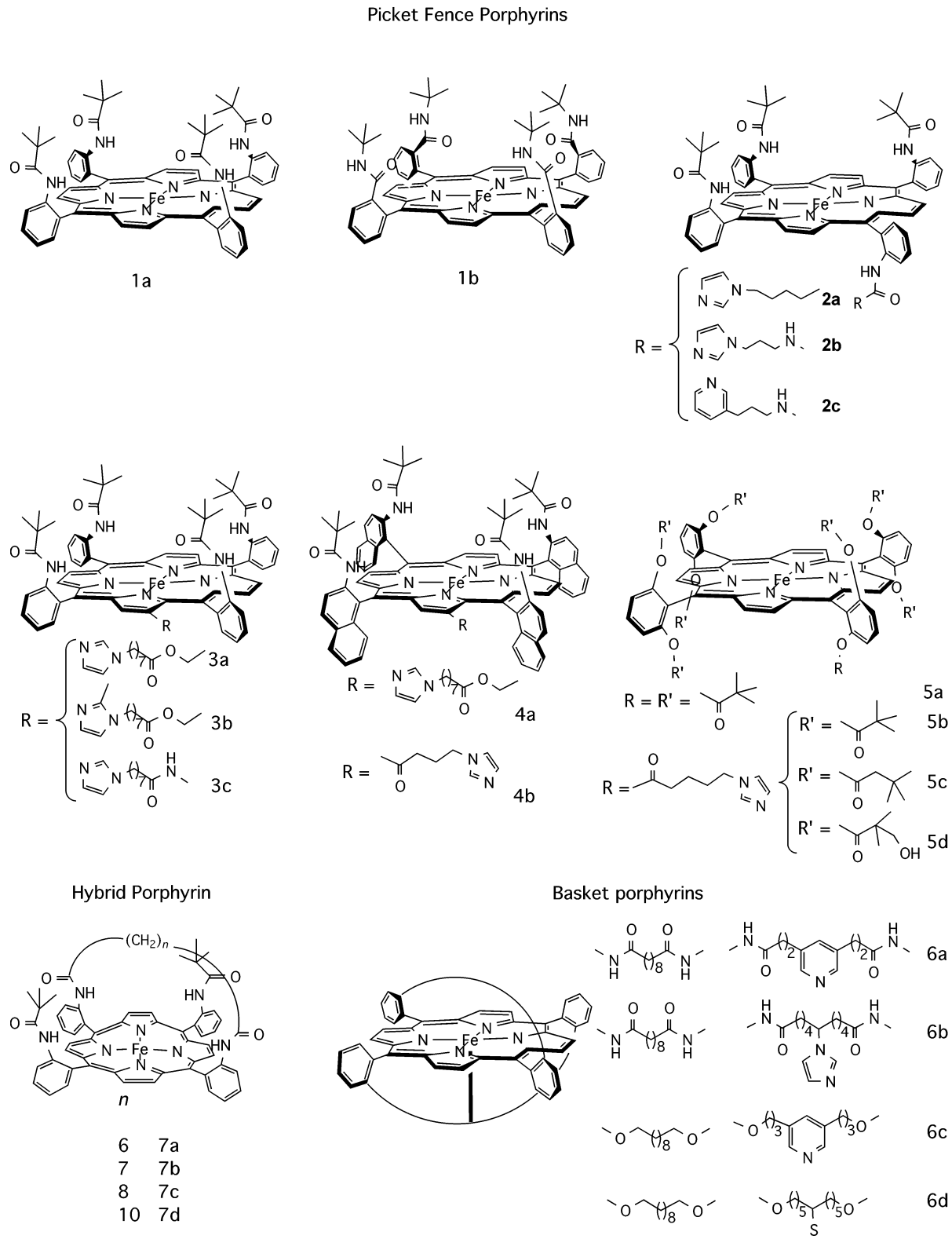

Figure 3. Biomimetic Mb analogues of the picket, hybrid, and pocket topologies reported since 1994 (**3**,[74] **4**,[75] **5d**,[77] and **6d**[79]) and select older compounds relevant in the context of the present discussion.

context of our review and for which LFER is most suitable, requires as inclusive a data set as possible.

The broad thermodynamic equivalency suggested by Figure 6A simplifies understanding the structure/activity relationship by expanding the set of compounds whose CO binding properties can be meaningfully compared. However, it also suggests that the existing Mb analogues are not likely to allow the understanding of the magnitude of relative contributions of steric and electronic factors to lowering the CO affinity of Mb and Hb. It is noteworthy that the same set of porphyrins is substantially more thermodynamically heterogeneous in O_2 binding, where at least four distinct groups can be identified.

The principally steric effects on the kinetics and thermodynamics of CO and O_2 binding can be exam-

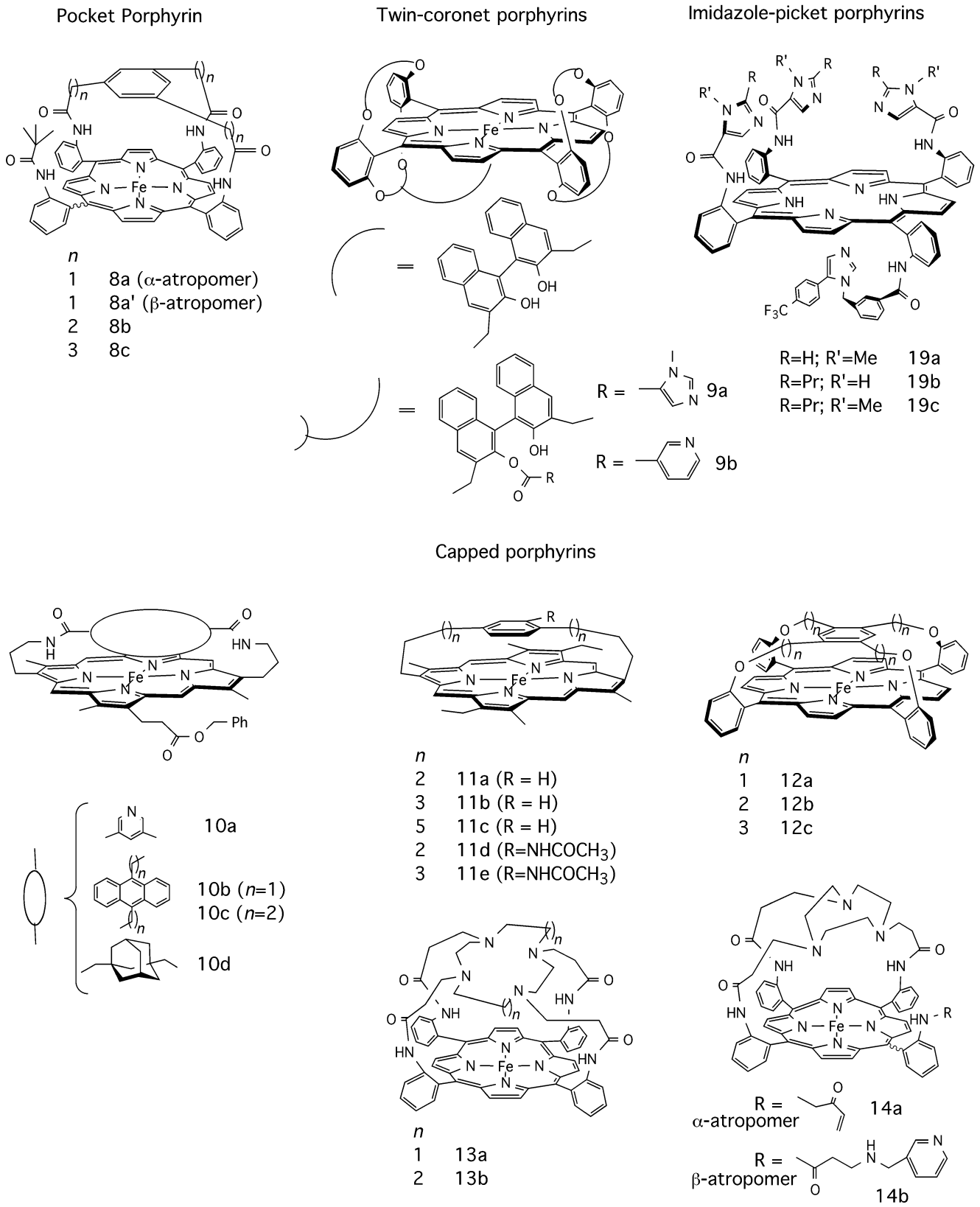

Figure 4. Biomimetic Mb analogues of the pocket, twin-coronet, and capped topologies reported since 1994 (**9**, **11**,[68,82] **12d**,[69] **13**, **14**,[66] and **19**[84]) and select older compounds relevant in the context of the present discussion.

ined in three homologous series of three or more compounds (**7**, **8**, and **11**). These series were designed to limit structural variations to a single parameter, the number of CH_2 units linking the cap and the porphyrin. It is likely that the relationship among the lowest-energy conformations of the homologues is not simple. For example, the binding-pocket size in **8** and **11** may be determined by the $\pi-\pi$ interaction between the porphyrin and the aryl cap more than by the linker length. Likewise, the degree of porphyrin ruffling, pronounced in **7a**,[68] probably varies noticeably within the series. However, the

Table 1. Kinetic and Thermodynamic Parameters of CO, and for Comparison Those of O_2, Binding to Biomimetic Analogues of Myoglobin[a]

	CO			O_2					
	k_+, M^{-1} s^{-1}	k_-, s^{-1}	$p_{1/2}$, Torr	k_+, M^{-1} s^{-1}	k_-, s^{-1}	$p_{1/2}$, Torr	M	conditions	ref
Mb	$3-5 \times 10^5$	$1.5-40 \times 10^{-3}$	0.014−0.025	$1-2 \times 10^7$	10−30	0.37−1	20−40	phosphate pH 7 buffer, 25 °C	71
Hb, human, R state	4.6×10^6	9×10^{-3}	1.4×10^{-3}	3.3×10^7	13.1	0.22	150	phosphate pH 7 buffer, 25 °C	71
1(dmim)	1.4×10^6	0.14	8.9×10^{-3}	1.1×10^8	4600	38	4280	toluene, 25 °C	72
2a	3.6×10^7	7.8×10^{-3}	2.2×10^{-5}	4.3×10^8	2900	0.58	2.7×10^4	toluene, 25 °C	72
2b	2.9×10^7	0.014	4.9×10^{-5}	2.6×10^8	3900	1.26	2.6×10^4	toluene, 25 °C	73
2c	4.8×10^7	0.33	6.4×10^{-4}	3.0×10^8	1.9×10^5	52.2	7.6×10^4	toluene, 25 °C	73
3a	3.1×10^7			6.4×10^8	1.4×10^3	0.29		toluene, 25 °C	74
3b	2.9×10^6			1.6×10^8	4.6×10^4	38		toluene, 25 °C	74
3c	1.1×10^7			3.7×10^8	1.3×10^4	4.6		toluene, 25 °C	74
4	3.3×10^6		1.5×10^{-4}	2.4×10^7	5.0×10^3	18	1.2×10^5	toluene, 25 °C	75
5b	1.8×10^6		4.9×10^{-4}	2.7×10^7	2.4×10^3	13	3×10^4	toluene, 25 °C	76
5c	1.3×10^7		7.2×10^{-5}	6.3×10^7	1.2×10^3	2.5	3×10^4	toluene, 25 °C	76
5d	2.0×10^5			2.6×10^4	55	33.5		CH_2Cl_2, 25 °C	77
6a	3.5×10^7	0.03	9×10^{-5}	3.6×10^8	5000	2	2×10^4	toluene, 20 °C	78
6b	4.0×10^7	0.0067	1.7×10^{-5}	3.1×10^8	620	0.29	17000	toluene, 20 °C	78
6c	6.8×10^7	0.069	1×10^{-4}	3.0×10^8	4×10^4	18	1.8×10^5	toluene, 20 °C	78
6d	8.8×10^4	28	0.026	5.2×10^6	800	12.4	480	toluene, 20 °C	79
7a(dmim)	2.0×10^4	0.08	0.50	5.4×10^5	15	2.7	5.4	toluene, 20 °C	80
7b(dmim)	1.0×10^5	0.031	0.03	1.0×10^7	67	0.67	21	toluene, 20 °C	80
7c(dmim)	1.7×10^5	0.050	0.03	1.5×10^7	540	3.6	121	toluene, 20 °C	80
7d(dmim)	4.7×10^6	0.11	0.002	3.9×10^8	7500	1.9	827	toluene, 20 °C	80
7a(mim)	8.0×10^4	0.0082	0.01	2.2×10^6	2.0	0.07	7	toluene, 20 °C	80
7b(mim)	1.0×10^6	0.0026	2.6×10^{-4}	2.1×10^7	5.0	0.023	88	toluene, 20 °C	80
7c(mim)	1.8×10^6	0.002	1.1×10^{-4}	3.0×10^7	27	0.091	818	toluene, 20 °C	80
7d(mim)	6.3×10^7	0.0027	4.2×10^{-6}	6.2×10^8	130	0.02	5000	toluene, 20 °C	80
8a(mim)	5.8×10^5	8.6×10^{-3}	1.5×10^{-3}	2.2×10^6	9	0.36	270	toluene, 25 °C	72
8b(mim)	1.5×10^6	9.4×10^{-3}	6.5×10^{-4}	1.7×10^7	71	0.36	550	toluene, 25 °C	72
8a(dmim)	9.8×10^4	0.055	0.067	1.9×10^6	280	12.6	216	toluene, 25 °C	72
8b(dmim)	2.1×10^5	0.053	0.026	5.2×10^6	800	12.4	480	toluene, 25 °C	72
8c(dmim)			0.001	7.4×10^8	34500	4	3500	toluene, 25 °C	72
9a	2.1×10^7	0.23	1.1×10^{-3}	4.0×10^7	2000	1.3	1180	toluene, 25 °C	71
9b	1.6×10^7	3.2	1.7×10^{-2}	2.7×10^7	2500	9.4	550	toluene, 25 °C	71
10a(dcim)	6×10^2	0.24	37	1.1×10^4	68	540	14	toluene, 20 °C	81
10b(dcim)	3×10^4	0.05	0.17	1.0×10^5	800	700	4100	toluene, 20 °C	81
10c(dcim)	6×10^6	0.05	0.0009	6.5×10^7	1000	1.4	1500	toluene, 20 °C	81
10d(dcim)	1×10^4	0.05	0.57	1.5×10^5	690	300	530	toluene, 20 °C	81
11a(mim)	4.9×10^6	0.014	0.0015	1.0×10^7	10^4	∼100	$\sim 10^5$	toluene, 20 °C	82
11a(dcim)	3.0×10^6	0.7	0.023	8.2×10^7	10^5	∼150	∼6000	toluene, 20 °C	82
11b(dcim)	1.1×10^7	0.13	0.0012	1.0×10^8	10^5	∼70	7×10^4	toluene, 20 °C	82
11c(dcim)	1.0×10^6	0.014	0.015	1.0×10^7	10^4	∼150	$\sim 10^5$	toluene, 20 °C	82
12a(mim)	1.0×10^6	0.05	5×10^{-3}			23	4300	toluene, 25 °C	72
12a(dmim)			0.20			4000	2×10^4	toluene, 25 °C	72
12b(dcim)	4.1×10^6	0.17	4.1×10^{-3}					toluene, 25 °C	72
13a(dmim)			>3500			760	<0.22	toluene, 20 °C	66
13a(dcim)			>3500			∼760	<0.22	toluene, 20 °C	66
13b(dmim)			>3500			22	<0.006	toluene, 4 °C	66
13b(dcim)			>3500			∼3	<0.003	toluene, 20 °C	66
14a(dmim)			2.9			2.3	0.79	toluene, 20 °C	66
14b			1.5			3.7	2.5	toluene, 20 °C	66
16a(C_{12}mim)	3.9×10^6	0.14	0.028	2.8×10^8	1.5×10^4	32	1100	phosphate pH 7 buffer, 25 °C	29
17a(dmim)			0.35			0.035	0.1	toluene, 25 °C	83
17b(dmim)			0.19			0.016	0.08	toluene, 25 °C	83

[a] For chemical structures see Figures 3−5. dmim, 1,2-dimethylimidazole; mim, 1-methylimidazole; dcim, 1,5-dicyclohexylimidazole; C_{12}mim, 5-dodecyl-1-methylimidazole.

broad capacity of the binding pocket to accommodate the steric demands of a sixth ligand on Fe probably correlates positively with the linker lengths.

A strong positive correlation between the *M* value and the length of the cap/porphyrin linkers is clearly observed for all series (Table 2). This correlation further confirms the validity of the paradigm that purely steric discrimination against CO, based on different steric properties of the Fe−C−O and Fe−O−O moieties, is possible. However, while the steric hindrance in the binding pocket has a predictable and uniform effect on *M* values in these three series of Mb analogues, it has a variable influence on the kinetic parameters, particularly those of O_2 binding. Thus, the effect of sterics in CO vs O_2 discrimination appears to be more complex than a decrease in k_+(CO).

Single-crystal X-ray diffraction studies of CO-ligated sterically encumbered Mb models also clearly indicate that the expansion of the distal superstructure, sometimes accompanied by increased porphyrin nonplanarity, and not tilting or bending of CO, is the

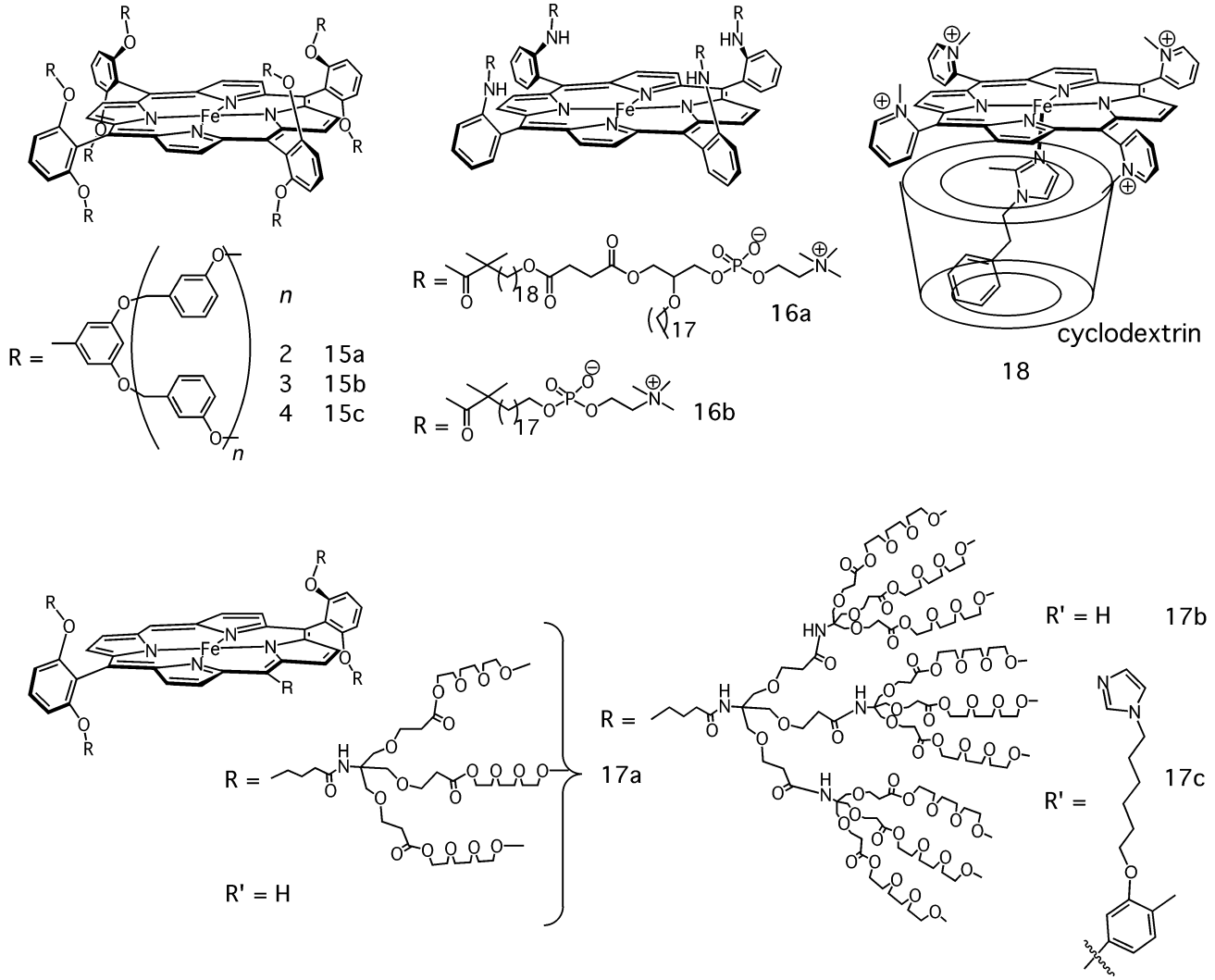

Figure 5. Dendritic, lipid-derivatized, and supramolecular analogues of Mb.[29,30,83,85,86]

Table 2. Correlation Coefficients for Homologous Series 7 (Four Homologues), 8 (Three Homologues), and 11 (Three Homologues)[a]

	CO			O_2			
series	k_+	k_-	$p_{1/2}$	k_+	k_-	$p_{1/2}$	M
7(mim)	*0.89*	*−0.68*	*−0.70*	*0.90*	*0.94*	−0.40	*0.93*
7(dmim)	*0.89*	0.55	*−0.72*	*0.89*	−0.53	−0.01	*0.93*
8(dmim)	no data	no data	*−0.99*	*0.87*	*0.87*	*−0.88*	*0.90*
11(dcim)	−0.37	*−0.85*	−0.18	*−0.87*	*−0.94*	0.19	*0.92*

[a] A positive value corresponds to an increase in the parameter with increasing length of cap/porphyrin linkers. Statistically meaningful coefficients are in italics.

predominant form of steric distortions (Figure 7). Minimal distortion of the Fe−CO unit in model compounds is also supported by extensive spectroscopic evidence.[89]

A less-recognized corollary of this observation is that the linear Fe−C−O moiety in CO adducts of Mb and Hb does not by itself rule out sterics as the major molecular mechanism of the discrimination. Spiro has discussed this issue in detail and ruled out steric effects.[25] However, in our opinion, this conclusion is based too heavily on computational results, as the number of mutants studied is still too small to reasonably claim that all possible ways to induce and/or distribute strain upon CO binding have been probed.

The effects of polarity (electrostatic potential) and of H-bonding within the binding pocket, while studied extensively in Mb and Hb, and currently thought to be at least as important as sterics in determining the M values of globins,[21,23,25] have been relatively little examined in Mb models. Kinetic and thermodynamic data on CO and O_2 binding exist for three pairs of synthetic porphyrins (**10a** vs **11c**; **14b** vs **8b**(mim); **9a** vs **4**) with pockets of comparable sizes but of significantly different polarities. The latter correlates with the C−O and Fe−C stretching frequencies and ^{13}C NMR chemical shifts of the CO adducts.[83] In the most dramatic example (**10a**, $M = 14$ vs **11c**, $M = 10^5$), the amide and pyridinyl moieties of the binding pocket in **10a** appear to cause $>10^4$-fold reduction in the M value. Relative to **11c**, the $k_+(CO)$, $k_+(O_2)$, and $k_-(O_2)$ values in **10a** are 10^2-10^3 times lower, whereas $k_-(CO)$ is 20-fold higher. An increase in the k_- value is often interpreted as an indicator of electronic destabilization of the bound ligand. However, the origin of lower $k_+(CO)$, $k_+(O_2)$, and $k_-(O_2)$ is not known, as such a relative decrease cannot be attributed to steric factors. Substantially higher selectivity toward O_2 binding is observed in **14b**, whose

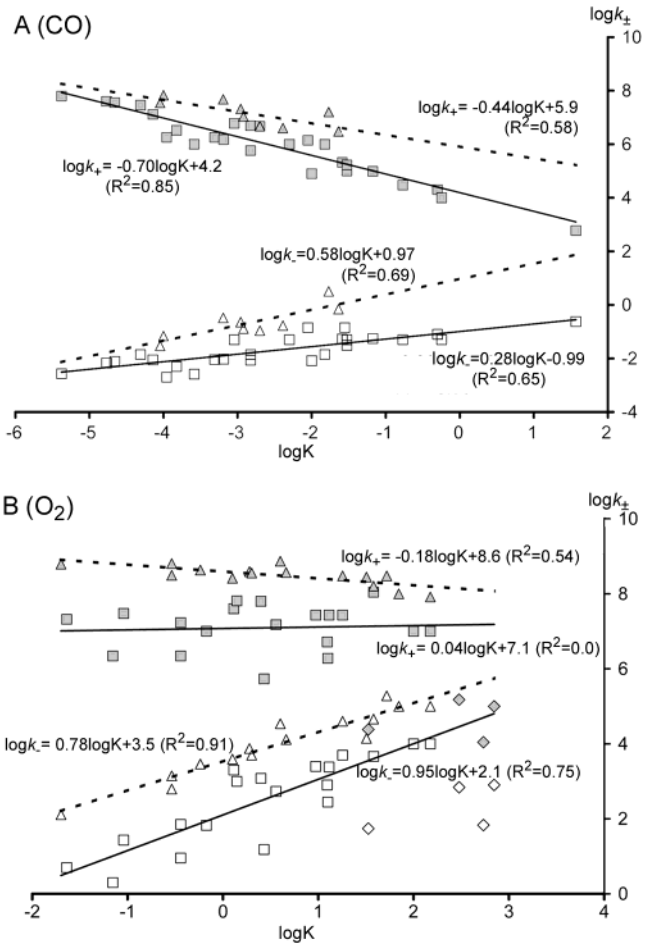

Figure 6. Linear free-energy relationship (LFER) for CO (A) and O_2 (B) binding to biomimetic Mb analogues. Signs with the gray background, k_+; signs with the white background, k_-. (A) triangles, group 1; squares, group 2. (B) triangles, group 1; squares, groups 2 and 3; diamonds, group 4. The least-squares fits (broken lines, group 1; solid lines, group 2) were performed to the following LFER equations: $\log k_+ = k_0 - \alpha \log p_{1/2} - \log H$ and $\log k_- = k_0 - (\alpha - 1) \ln p_{1/2}$, where H is Henry's constant (0.96×10^{-5} Torr^{-1} M for CO and 0.72×10^{-5} Torr^{-1} M for O_2 in toluene at 25 °C). Data reported at other temperatures were adjusted to 25 °C. The parameter α (the slope of the log k vs log K graphs) is the contribution of the free energy of the reactants to the free energy of the transition state. Assignment of porphyrins into different groups was performed by maximizing $\sum_i (\rho^i_{\log k_+, \log K} + \rho^i_{\log k_-, \log K})$ for both groups, where $\rho_{X,Y}$ are the correlation coefficients and i is the group number. Very low slopes of the log $k_{on}(O_2)$ vs log $K(O_2)$ dependence preclude statistics-based grouping. Data used to create the figures are available as Supporting Information.

tacn-defined binding pocket is somewhat larger but more polar than that in **8b**(mim) (Figure 8) and whose M value (2.5) is >200 times less ($M_{\mathbf{8b}(\mathrm{mim})} = 550$). Hydrogen bonding to bound O_2 was invoked to rationalize the lower M values of **9a** relative to those of the sterically comparable **4**.[71]

In contrast to the stereoelectronic properties of the binding pocket, the nature of the proximal ligand—imidazole vs pyridine (**6a** vs **6b**; **9a** vs **9b**; and **2b** vs **2c**), or 1-MeIm vs 1,2-Me_2Im (**7**, **8** and **12a**)—appears to have a limited effect on the M values. However, in a single example, thiolate was found to increase the selectivity by a factor of 400 (**6d** vs **6c**, Table 1).

Table 3. O_2 Affinity of Select Mb Models Capable of Forming an H-Bond to Bound O_2 and Their Analogues Lacking Accessible H-Bond Donors[a]

accessible H-bond donor	$p_{1/2}$, Torr	ref	analogue without H-donor	$p_{1/2}'$, Torr	ref	H-bond effect: $p_{1/2}/p_{1/2}'$	H-bond effect: ΔΔG, kcal/mol
2a	0.58	72	**5b**	13	76	30	2.0
3a	0.29	74					
6a	2	78	**6c**	18	78	9	1.3
11a	9.5	82	**11d**	55.7	82	6	1.1
11b	2.8	82	**11e**	22.7	82	8	1.2
5d	33.5	77	**5c**	2.5	76	0.07	−1.6

[a] The same conditions as those cited in Table 1, except for compounds **11** (toluene, −45 °C).[68]

By the LFER criterion, **6d** is an outlier among the porphyrins in Table 1.

Recently reported dendritic porphyrins **17a** and **17b** bind O_2 in preference of CO by a factor of >10, even though they lack rigid, centrally positioned superstructures.[83] Both the unusually high O_2 affinity, presumably assisted by a H-bond between an amide group and bound dioxygen (see below), and the relatively low CO affinities contribute to the very low M values of these porphyrins.

2.2.2. Electrostatic and H-Bonding Effects on Heme's Affinity for Small Molecules

Dipolar interactions with distal amino acids, particularly the H-bond between the imidazole residue of distal histidine and oxygen atoms of oxyheme, are estimated to enhance O_2 binding to Mb and Hb by a factor of 10^3 (which is partially compensated by endergonic displacement of H_2O required for O_2 binding).[21] The hydrogen bond not only favors O_2 binding but also is thought to stabilize oxyheme against superoxide-releasing autoxidation and contribute to CO vs O_2 discrimination. However, the electronic effects within the binding pocket of globins on heme's ligand affinities remain poorly understood, in large part because it is impossible to replace a single amino acid and leave the rest of the protein unchanged and because of the dearth of high-resolution structural data on such mutants. Hence, biomimetic analogues, which are more amenable to precise structural modification and spectroscopic characterization, could conceivably be particularly useful in probing these issues. Yet, it has been difficult to design reversibly O_2-binding porphyrins with suitably positioned H-bond donors. The existence of relatively weak H-bonds, especially between anilidine groups of the porphyrin ligand and coordinated O_2, is now established.[22] Five pairs of structurally similar porphyrins are available wherein only one member can form a H-bond to coordinated O_2 (Table 3). With one exception, the compound with an accessible H-bond donor has O_2 affinities 10−30 times higher than those of the analogue lacking an H-bond donor. In **6a**, the existence of a H-bond between the amide group and coordinated O_2 was demonstrated by low-temperature proton and ^{17}O NMR, IR, and Raman spectroscopies.[78] The higher O_2 affinity of **6a** vs **6c** is mainly due to the lower dissociation rate constant in **6a**, which was interpreted as additional evidence

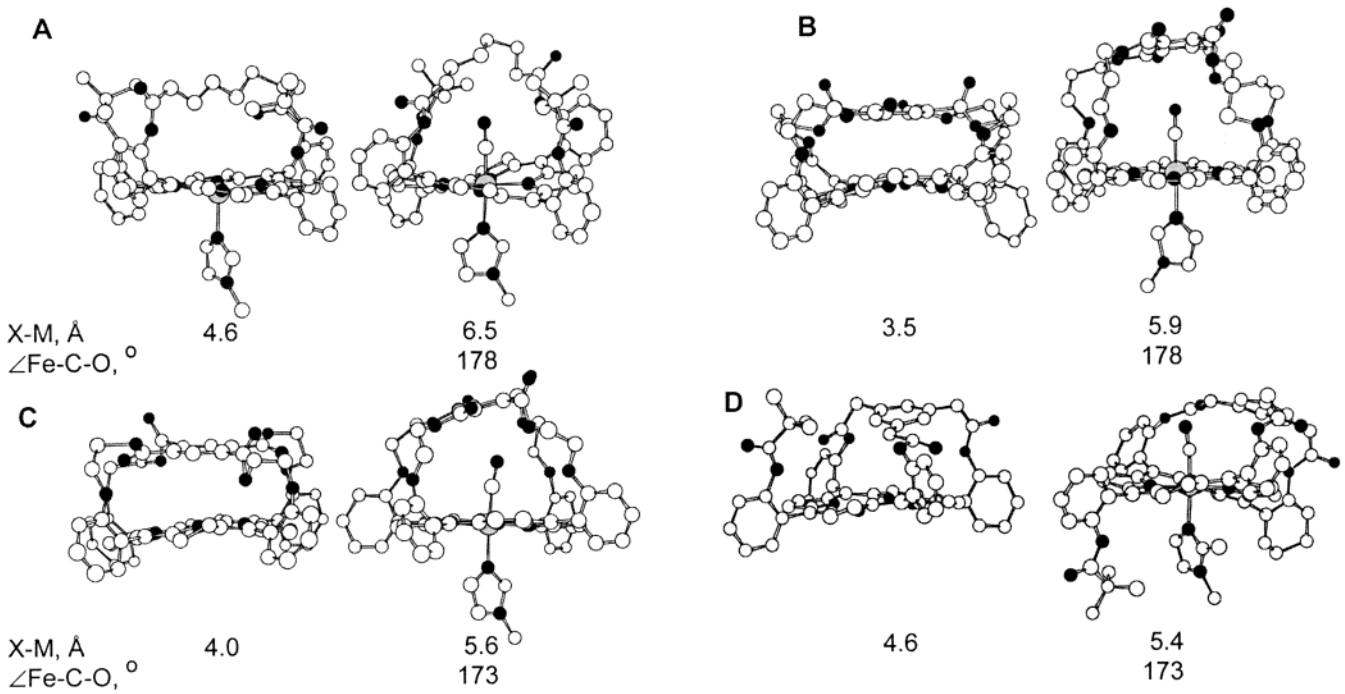

Figure 7. Single-crystal X-ray diffraction structures of (A) **7a**(mim)(CO), (B) **12c**(mim)(CO), (C) **12b(**mim**)**(CO), and (D) **8a′**(mim)(CO) and for comparison, structures of **7a**(mim) (A), the corresponding free bases (B,C), and the α_4 atropomer of the corresponding free base (D). X−M is the distance between the centroid of the distal superstucture and Fe (or the porphyrin centroid for free bases). Major conformational distortions upon CO binding include vertical (A−C) and lateral (D) displacements of distal superstucture and porphyrin ruffling (A). For chemical structures, see Figures 3 and 4. The listed metric parameters are from refs 24 and 80. Generated using Chem3D from CCDS coordinate files GAJHAA,[90] YIMYOU[80] (A); ZUMRAA,[70] ZUMREC[70] (B); PYROPR,[91] JIXNAF[92] (C); and ZUMQUT,[70] SAHCAF[93] (D).

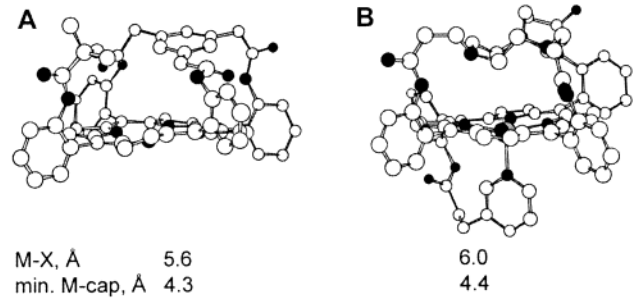

Figure 8. Single-crystal X-ray diffraction structures of (A) the free base for **8b** and (B) an analogue of **14b**. M−X is the distance between the metal (porphyrin centroid for A) and the centroid of the cap; min. M−cap is the the shortest contact between the metal (porphyrin centroid for A) and the cap. On the basis of both parameters, **14b** has a less sterically congested cavity, yet it manifests higher $p_{1/2}$(CO) and lower *M* than **8b**. Generated using Chem3D from CCDS coordinates ZUMQUT[70] and GIXJOM.[94]

for stabilization of the O_2 adduct. In contrast, the higher affinities of **2a** and **3a** relative to **5b** are due mainly to the lower k_+ of the latter. In all cases, the H-bond contributes <2.0 kcal/mol of stabilization; this relatively low value was taken as an indication that the spatial arrangement of the H-bond donor and O_2 is nonoptimal.[22] In contrast to the above examples, one of Tsuchida's porphyrins, bearing OH-modified pivalyl ester pickets (**5c**),[76] has an O_2 affinity >10 times lower than that of the analogous compound with aliphatic pickets (**5d**);[77] no explanation for this unusual fact was proposed. The quantitative comparison is complicated because the $p_{1/2}$ of **5d** was measured in CH_2Cl_2, whereas that of **5c** was measured in toluene. However, the more polar solvent likely increases the O_2 affinity of **5d**, thereby decreasing the $p_{1/2}/p_{1/2}'$ ratio, which would probably be even smaller if the measurements could be carried out in a single solvent.

The effect of introducing additional H-bond donors into picket-fence porphyrins was examined by Reed and co-workers;[95] they observed a maximum 9-fold stabilization of the O_2 adduct. Collman et al. reported a series of "picnic-basket" porphyrins, wherein the O_2 affinity correlated qualitatively with the length of a strap connecting two pairs of anilidine moieties.[96] It was hypothesized that the longer straps pushed the anilidine groups away from the coordinated O_2, increasing the O···HN distance and hence weakening the H-bond. A remarkable (10^2−10^4-fold) increase in the O_2 affinity of Co porphyrins was observed by Chang et al. upon the introduction of a carboxylic acid moiety at a distance suitable for formation of H-bonding with Co-coordinated O_2.[97]

Despite some progress, the studies of biomimetic Mb analogues with H-bond donors in the vicinity of coordinated O_2 are complicated by the apparent susceptibility of such compounds to undergo rapid superoxide-releasing autoxidation whenever the pK_a value of the H-bond donor is within the biological range.[68,77,81,95] This contrasts with the proposed role of the distal imidazole in Mb and Hb of *stabilizing* oxyheme against autoxidation.[26]

The unusually high O_2 affinities of dendritic porphyrins **17** were suggested to indicate a strong H-bond between the amide NH group and bound O_2.[83] Strong H-bonding in these compounds seems somewhat surprising. First, the existence of appreciable H-bonding between the distal O atom of coordinated

O_2 and the anilidine group of tetraaminophenylporphyrin (TAPP, compounds **1a**, **2**, **3**, **6a**) and the apparent lack of such stabilizing polar interactions in "inverted" picket-fence porphyrins (**1b**) define the range of $Fe-N_{amide}$ distances that may be optimal for H-bonding to bound O_2 in TAPP-based Mb analogues. In **17**, the amide NH groups are separated from the phenyl groups of the TAPP platform by four additional carbon atoms. While the flexible linker could conceivably adopt a conformation that would bring the NH groups closer to coordinated O_2, such conformation is not sterically favorable, since the NH moieties are directly connected to a tertiary center. Second, adoption of such a conformation is likely associated with a significant entropic penalty. Third, H-bonds between the NH groups and the O atoms at the base of the first dedritic shell create thermodynamically favorable five-membered rings and hence would effectively compete with H-bonding to coordinated O_2 with lower entropic and steric penalties. It therefore appears that understanding the fascinating high O_2 affinity of dendritic porphyrins **17** requires further study.

Interesting albeit qualitative data were recently reported by Collman et al. on O_2 affinities of imidazole-derivatized Co tetraarylporphyrins, **19** (Figure 4).[98] The Co rather than the Fe derivatives were used because the higher stability of $Co-O_2$ adducts and their $S = {}^1/_2$ spin state make oxycobalt porphyrins amenable to magnetic studies. Most studies were carried out on **19c**Co derivatives, but **19a**Co analogues behave similarly.

As expected of an imidazole-ligated five-coordinate porphyrin, **19c**Co reversibly forms an O_2 adduct, **19c**CoO_2, best described as a Co−superoxide complex. Oxygenation was followed by visible absorption and EPR spectroscopies, and the product was further characterized by oxygen-isotope-sensitive bands in the resonance Raman spectra. In CH_2Cl_2, **19c**Co manifests a visible spectrum characteristic of a five-coordinate Co^{II} porphyrin (the Soret band at λ_{max} 416 nm which moves to 443 nm upon exposure of the solution to 1 atm O_2). The EPR spectrum of **19c**Co is consistent with identification of this species as a Co(por) with an axial nitrogen ligand. Upon exposure to dioxygen, a new EPR signal is observed corresponding to the expected metalloporphyrin superoxide, **19c**CoO_2; this spectrum is very similar to that of $CoMbO_2$ and other oxygen-binding cobaltohemes. A band at 1148/1077 cm^{-1} ($^{16}O_2/^{18}O_2$) in the resonance Raman spectrum of **19c**CoO_2 corresponds to an O−O bond stretch of a Co(por)−superoxide complex.

Oxygenation of the bimetallic **19c**Co/M complexes (M = Ag^I, Cu^I, Zn^{II}) generates a superoxide derivative, based on its EPR and oxygen-isotope-sensitive resonance Raman (ν_{O-O}, 1143/1070 cm^{-1},$^{16}O_2/^{18}O_2$) spectroscopies. Despite the apparent lack of any steric impediment for formation of a $Co^{III}-O-O-Cu^{II}$ bridged peroxo species, such intramolecular electron transfer does not occur, and the adduct exists as an O_2^-/Cu^I redox isomer. While the presence of the distal metal apparently has little effect on the amount of electron density on bound O_2 (as judged by the O−O frequency), it decreases $k_-(O_2)$ so significantly that the O_2 adducts do not deoxygenate, even upon prolonged exposure to dynamic vacuum (<5 mTorr). The EPR spectra of **19c**CoO_2/M (M = Ag^I, Cu^I, Zn^{II}) have significantly more pronounced hyperfine structures than that of **19c**CoO_2, suggesting that O_2 in **19c**CoO_2/M has less $Co-O_2$ rotational freedom than in **19c**CoO_2. The hyperfine structure of the superoxide signal of **19c**CoO_2/Cu^I sharpens upon deuteration of the amide NH groups, demonstrating that there are discernible interactions occurring between the bound oxygen and amido-NH groups. In **19c**Co, no measurable difference in the hyperfine structure is observed upon deuteration of the amido NH groups. It was hypothesized that the greater dioxygen affinity of **19c**Co/M arises at least in part from structural changes in the ligand scaffold, induced by coordination of the distal metal ion, which stabilize the amide$NH\cdots O_2Co$(por) interaction. In effect, a distal metal ion preorganizes the metalloporphyrin structure into a high-affinity state, which may not be energetically accessible in the monometallic analogue. The positively charged distal environment may further stabilize the CoO_2 adduct through electrostatic interactions with the partial negative charge of the bound oxygen. This work clearly demonstrates the importance of electrostatic effects in the binding pocket on the affinity of small molecules to a metalloporphyrin. More recently, the dioxygen adducts of **19c**Fe and **19c**Fe/Cu have been shown to be ferriporphyrin−superoxide complexes in solution.[99] The dioxygen affinity and stability against irreversible oxidation are greatly increased by Cu^I.

2.2.3. Reversible Oxygen Carriers in Protic Media

The steric bulk of the globin moiety effectively prevents the bimolecular reaction between a ferroheme and an oxyheme, which is the dominant mechanism of irreversible aerobic oxidation of simple Fe^{II} porphyrins in solution. The protein also efficiently suppresses Fe−O bond heterolysis in oxyheme, a process that generates ferriheme with the release of superoxide, O_2^- (or hydroperoxyl radical, HO_2, if the oxyheme is protonated). The protective mechanism of the globin in the latter reaction is not well understood, but the hydrophobic, water-poor environment of the O_2-binding pocket is thought to be important. Such a property was built into all but one reported-to-date synthetic porphyrin-based systems that bind O_2 reversibly in the presence of water.

The earliest example is that of Tsuchida based on picket-fence-type porphyrins embedded in phospholipid vesicles[76] or lipid-derivatized tetrakis(*o*-aminophenyl)porphyrins, **16** (Figure 5).[28,29,85,100] In aqueous media, this so-called lipidporphyrin assembles into unilamellar vesicles of ~100 nm diameter. In the presence of a slight molar excess of dodecylimidazole (C_{12}im) or 5-dodecyl-1-methylimidazole (C_{12}mim), an O_2Fe(porphyrin) adduct is formed reversibly. The lipid environment significantly retards the autoxidation rate (Table 4) but apparently has little effect on the kinetics of O_2 and CO binding, suggesting the lack of barriers for O_2 or CO diffusion through the lipid layer. Faster autoxidation in the presence of C_{12}-im, which favors formation of the bis-imidazole

Table 4. Reversible O_2 Carriers under Protic Conditions[a]

	solvent	$p_{1/2}(O_2)$, Torr	$\tau_{1/2}$, h	ref
Hb, human, α chain	H_2O pH 7	0.22	>60	71
5b/dpmc (vesicles)[b]	H_2O pH 7	37	>36	76
15a(mim)	toluene/H_2O		1.5	30
15b(mim)	toluene/H_2O		6	30
15c(mim)	toluene/H_2O		3×10^8	30
16a(C_{12}mim) (liposome)	H_2O pH 7.4	32	50	29
16a(C_{12}im) (liposome)	H_2O pH 7.4	30 (at 37 °C)	17	28, 29
16b (as "fibers")	H_2O pH 7	25	4	85
17b(mim)	toluene/H_2O	0.016 (in dry toluene)	2	83
18	DMF/H_2O		0.7 (5 °C)	27

[a] dpmc, 1,2-bis(myristoyl)-*sn*-glycerophosphocholine; mim, 1-methylimidazole; dmim, 1,2-dimethylimidazole; C_{12}im, 5-dodecylimidazole; C_{12}mim, 5-dodecyl-1-methylimidazole. [b] **5b**:dmpc ratio 1:1000.

adduct, may be due to imidazole-assisted displacement of O_2^-. Although the assemblies manifest an exponential (non-cooperative) oxygenation curve, as expected, they were reported to have O_2-transporting efficiencies (defined as the difference in the fraction of oxygenated and deoxygenated complex under the O_2 tensions in lungs and muscles) comparable to that of human erythrocytes (20% vs 22%).[28]

Aida's group reported a family of dendritic Fe porphyrins (**15**, Figure 5).[30] Every member binds O_2 reversibly in anhydrous toluene; in toluene/H_2O mixtures (1000 equiv of H_2O relative to the porphyrin) the stability toward autoxidation correlates with the size of the dendritic shell. The highest-generation member was claimed to be incredibly resistant to autoxidation ($k_{app} \approx 3 \times 10^{-9}$ h^{-1}!). Unlike the lipid system, the dendritic shell significantly slows diffusion of O_2 and CO. For example, under 1 atm CO, the dioxygenated porphyrin converts into the CO adduct with a half-life of 50 h.

Recently, Tsuchida and co-workers reported very preliminary results on reversible dioxygenation of an interesting supramolecular system comprised of phenethylimidazole-ligated tetrakis(*N*-methylpyridinium)-porphyrinatoiron(II) and cyclodextrin (**18**, Figure 5).[27] Irreversible oxidation of Fe^{II} was remarkably slow ($\tau_{1/2}$ = 40 min at 5 °C) and followed first-order kinetics, suggesting superoxide-releasing autoxidation as the dominant mechanism. It was hypothesized that the 4+ charge of the porphyrin prevents formation of peroxo-bridged porphyrin dimers and also suppresses the protonation of the distal O atom in the O_2 adduct, thereby slowing autoxidation.

2.3. Reversible Cooperative O_2 Carriers: Biomimetic Analogues of Hb

Cooperative ligand binding to polytopic receptors has been implemented in several synthetic systems.[101] Certain aspects of the molecular "trigger" of cooperative Hb oxygenation have also been demonstrated biomimetically, but the overall activating mechanism is yet to be reproduced outside the protein matrix. As a result, biomimetic chemistry has not contributed to understanding the mechanism of cooperativity in Hb, nor have the general principles that underlie cooperativity in Hb been utilized as a control mechanism in artificial systems.

Tsuchida et al. developed the first synthetic system to manifest cooperative O_2 binding using solutions of poly-L-lysine/heme assembly in aprotic solvents.[102] In the absence of O_2, the ferrous centers are six-coordinate, being ligated intramolecularly by two primary amines of the polylysine chain. Binding of O_2 replaces one of the coordinated amines, inducing a conformational change in the polymer backbone (which is manifested in a decrease in the helix content of the polymer). This is thought to sterically destabilize binding of the second amine ligand to other Fe porphyrins, inducing a switch of hemes throughout the polymer from the six-coordinate to the five-coordinate state, which has higher O_2 affinity. Oxygenation was claimed to be fully reversible, but the system required dithionate, which is a commonly used reductant for converting ferric to ferrous hemes. Autoxidation of oxyheme is probably facilitated by displacement of O_2^- with amine. Cooperative binding of CO and CN^- to these heme-modified polymers was also observed.

Soon thereafter, O_2 uptake by polycrystalline adducts of ferrous picket-fence porphyrin **1a** (Figure 3) and 2-methylimidazole or 1,2-dimethylimidazole (dmim) was found to be cooperative, with Hill coefficients of 2.6 and 3, respectively.[103] The system is robust, retaining cooperativity even after 50 oxygenation/deoxygenation cycles. The mechanism of cooperativity remains, however, unknown. The different O_2 affinity of the material at low and high O_2 tensions was ascribed to two distinct polymorphs. However, in the absence of any structural data on these polymorphs, it is impossible to know whether such presumed polymorphism is also associated with structural changes within individual molecules. Nevertheless, the speculation that the phase transition is triggered by a 5% decrease in a linear dimension of the ferroheme/imidazole adduct upon O_2 binding is plausible. However, the possibility that other conformational changes induce the phase transition cannot be ruled out. The cooperative O_2 uptake by these solids was likened to spin-crossover systems, wherein a sharp cooperative transition from one spin state to another occurs upon temperature change.[104] Such a cooperative spin transition depends on crystal size, counterion, solvate molecules, and defect content; nucleation and domain growth are thought to determine the kinetics of the transition. Indeed, crystals of **1a**(dmim) suitable for X-ray diffraction studies could only be grown as an ethanol solvate, which uptakes O_2 non-cooperatively. Removal of

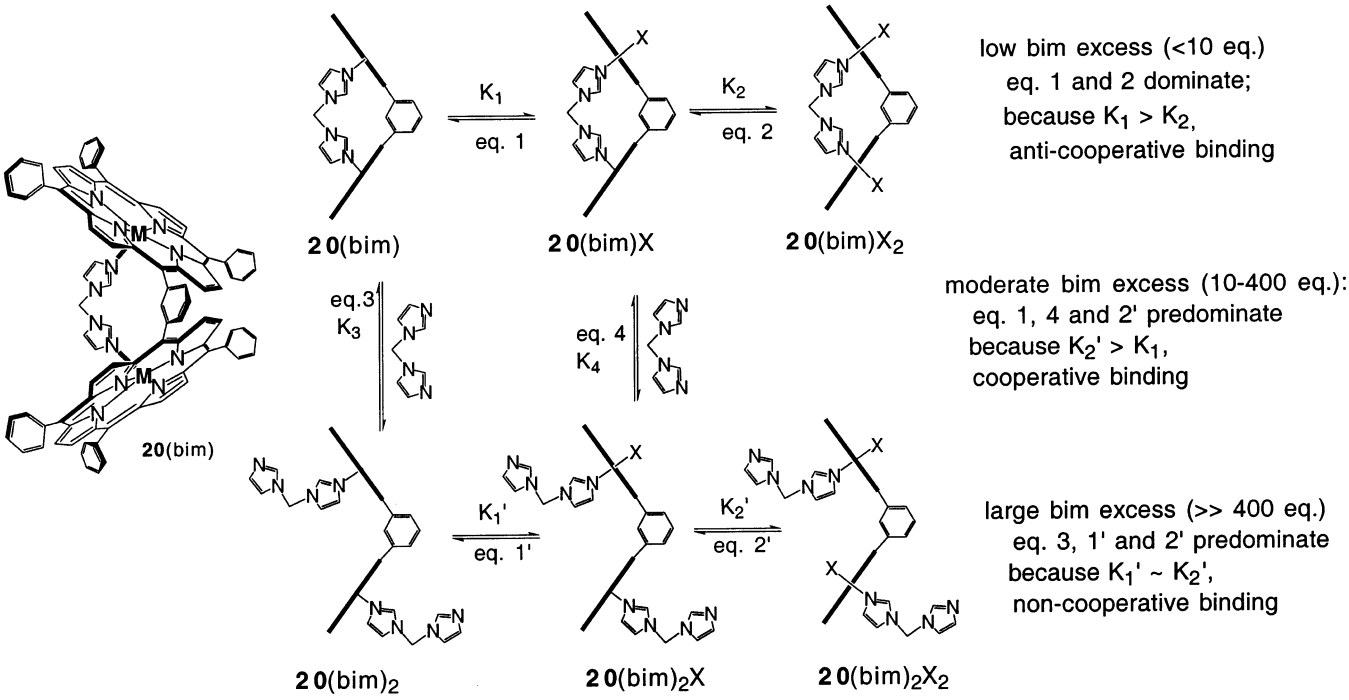

Figure 9. Gable porphyrin **20** and the set of equilibria that results in cooperative binding of X (O_2 or CO).

EtOH under vacuum regenerates the microcrystalline solid, manifesting the cooperativity.[104]

Bayer claimed cooperative O_2 binding to a heme-containing polymer,[105] but these results are now considered erroneous, mainly because the reported UV−vis spectra of what was thought to be dioxygen adducts do not correspond to spectra of any known dioxygenated Fe porphyrins.[22,103]

Cooperative binding of O_2 to the Co and of CO to the Fe derivatives of the so-called "gable" porphyrin was reported by Tabushi and co-workers.[106−108] Cooperativity appears to arise from perturbation, by O_2 or CO (X), of an equilibrium between metalloporphyrins containing one and two bisimidazolylmethane (bim) ligands (Figure 9). In **20**(bim), bim constrains the metal ions into the out-of-plane position, which disfavors the formation of six-coordinate sites. This decreases the binding affinity of X (K_1), because the in-plane movement of the metal necessary for the formation of a six-coordinate site introduces strain (estimated to be ~1.2 kcal/mol for the Co/O_2 system) into the molecule. This additional strain is relaxed in equilibrium 4, resulting in $K_3 < K_4$. As a result of this difference, a range of bim concentrations exists where compounds **20**(bim) and **20**(bim)$_2$X are favored over **20**(bim)$_2$ and **20**(bim)X in equilibria 3 and 4, respectively. Because $K_1 < K_2'$, under these conditions formation of **20**(bim)$_2$X$_2$ from **20**(bim) is cooperative. At sufficiently low concentrations of bim, equilibrium 2 remains more favorable relative to the sequence of equilibria 2′ and 4, despite $K_2' > K_2$, and formation of **20**(bim)$_2$X$_2$ is anti-cooperative. Likewise, at high bim concentrations, equilibrium 3 becomes important, so that **20**(bim)$_2$ is substantially populated, and **20**(bim)$_2$X$_2$ is formed from **20**(bim) non-cooperatively, primarily via equilibria 3, 1′, and 2′. Such concentration dependence was indeed observed experimentally. Depending on the values of K_3 and K_4, as much as 100-fold excess of bim is required to observe cooperative binding. Thus, even though cooperativity in gable porphyrins partially mimics the "trigger" mechanism of cooperativity in Hb, it is not an adequate biomimetic analogue of such a mechanism because of its basis in additional ligation equilibria.

3. Functional Analogues of the Heme/Cu_B Site of Cytochrome c Oxidase

3.1. The Enzyme

Cytochrome *c* and ubiquinol oxidases belong to a superfamily of heme/Cu terminal oxidases,[14] enzymes responsible for coupling the oxidation of ferrocytochrome *c* or ubiquinol, respectively, to the $4e^-/4H^+$ reduction of molecular oxygen. This is the final step in respiration, ferrocytochrome *c* and ubiquinol being the most oxidizing electron carriers of the respiratory chains in eukaryotes and certain prokaryotes, respectively. In addition to clearing the respiratory chain of low-energy electrons, heme/Cu terminal oxidases also contribute to maintaining the transmembrane electrochemical proton gradient by actively translocating protons. No attempts have been made to mimic the "proton pumping" capacity of heme/Cu terminal oxidases, and this aspect of the enzymatic reactivity will not be discussed in this review.

There is a rather close structural similarity among CcO's from different organisms,[109] and also between CcO and ubiquinol oxidase.[110] In all enzymes, O_2 is reduced at a bimetallic heme/Cu site (Figure 10) whose Fe−Cu distance varies slightly around 5 Å, depending on the exogenous ligation of the metals. Most known forms of heme/Cu terminal oxidases appear to undergo post-translational modification, resulting in a covalent bond between one of the Cu-ligating imidazoles and a tyrosine residue.[111a] The existence of this link is considered as evidence for

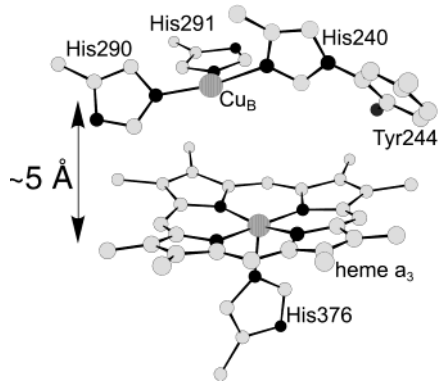

Figure 10. Catalytic site of bovine heart cytochrome *c* oxidase.[35] Carbon is gray, N and O atoms are black, and Fe and Cu are dark gray. The peripheral substituents of the heme are omitted for clarity.

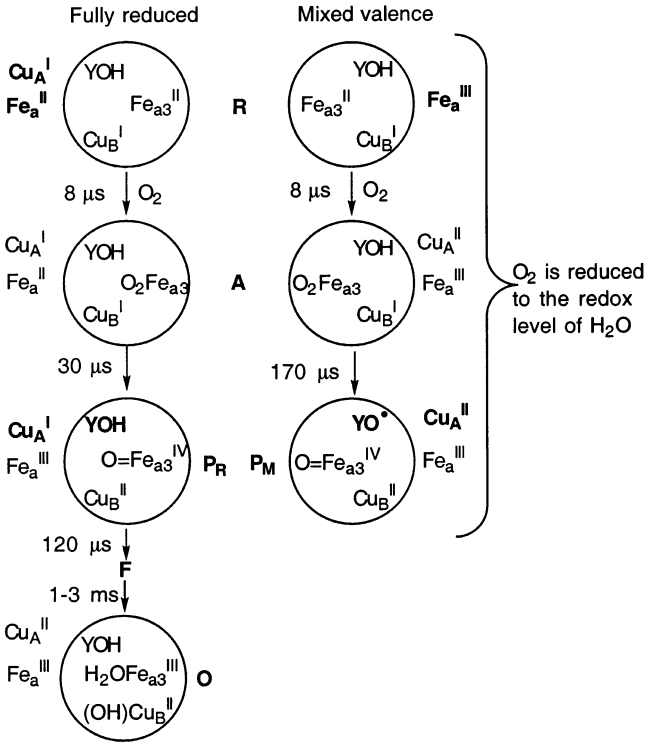

Figure 11. Spectroscopically observed intermediates (with their trivial names) in single-turnover reduction of O_2 by the fully reduced and mixed-valence forms of cytochrome oxidase.[112] Only the heme/Cu site (in circles) and the electron-transfer cofactors are shown; the nature of the fourth (exogenous) ligand at Cu_B is controversial, and the ligand is omitted. YOH = tyrosine. Cofactors whose redox states are different in corresponding intermediates derived from the fully reduced and mixed-valence forms are highlighted in bold.

the formation of the tyrosine radical during catalytic turnover.[111b] In addition to the bimetallic site, heme/Cu terminal oxidases contain between one and three other redox cofactors, such as bimetallic Cu_A and heme(s), whose functions are electron storage and electron transport from the external reductant to the catalytic site.

The nature of intermediates in O_2 reduction by CcO depends on the redox states of these cofactors (Figure 11). Whereas the heme/Cu site must be in the ferrous−cuprous state to bind O_2, other cofactors may be fully oxidized (the mixed-valence enzyme) or contain one or more external reducing equivalents. One of the most fascinating aspects of CcO's dioxygen reactivity is the enzyme's ability to reduce O_2 to the redox level of water on a much shorter time scale (<0.2 ms by the mixed-valence enzyme and 0.03 ms by the fully reduced enzyme)[112] than that on which CcO receives an electron from ferrocytochrome *c* (5−20 ms).[1] Such a decoupling of the O_2 reduction kinetics (the R → P transformation, Figure 11) from that of electron transport within the respiratory chain conceivably minimizes the lifetime of catalytic intermediates containing partially reduced oxygen species, and therefore the possibility that such a species is released into the medium. Two phenomena contribute to this decoupling: (i) the inertness to O_2 of the redox forms of CcO that do not contain enough electrons to reduce O_2 to the redox level of H_2O and (ii) the capacity of the protein matrix to temporarily store an oxidizing equivalent derived from O_2 (e.g., as a Tyr244 radical, Figure 10).[111]

Although such very rapid reduction of O_2 is biologically beneficial, the absence of any spectroscopically detectable intermediates between compounds A and P substantially complicates unraveling the fundamental question of how the O−O bond is reduced at the heme/Cu site. One issue that has particularly fascinated the biomimetic community is how much this facile O_2 reduction is due to the presence of Cu_B. Single-turnover experiments with CcO indicate[11] that reduction of O_2 is coupled to oxidation of Cu_B (although the biological relevance of this observation was questioned[33]), but whether Cu_B lowers the activation barrier of O_2 reduction (for example, by forming a transient $Fe^{III}-O-O-Cu^{II}$ intermediate) or serves mainly as an electron storage site in a close proximity of the O_2-reducing heme remains unknown. It was hypothesized[13,126b] that the μ-peroxo intermediate would facilitate O−O bond cleavage and/or stabilize the peroxo moiety against dissociation. A limited number of studies[113−119] demonstrated that Cu_B-free mutants of heme/Cu terminal oxidases retain intramolecular electron-transfer rates but do not catalyze O_2 reduction. On the basis of DFT calculations, O_2 reduction was proposed to proceed via a ferric−hydroperoxo intermediate generated by a hydrogen-atom transfer from a Cu_B^I-bound H_2O molecule. The resulting Cu_B^{II} may or may not interact with the distal OH moiety of this $Fe^{III}-OOH$ intermediate.[120]

A major advantage of the biomimetic approach for understanding the role of Cu_B lies in the fact that synthetic CcO analogues can be readily prepared in both the bimetallic FeCu and Cu-free forms, which either lack a distal metal or have a distal metal ion other than Cu. The reactivity of these forms under a broad range of conditions can be studied and compared to identify effects specific to Cu and, possibly, those caused by other distal metals. This strategy has been implemented within two largely complementary approaches. One approach, described elsewhere in this issue by Karlin,[40] involves studying stoichiometric reactions of reduced heme/Cu analogues with O_2 under nonprotic conditions. Suppressing acid−base reactions and utilizing temperatures lower than those

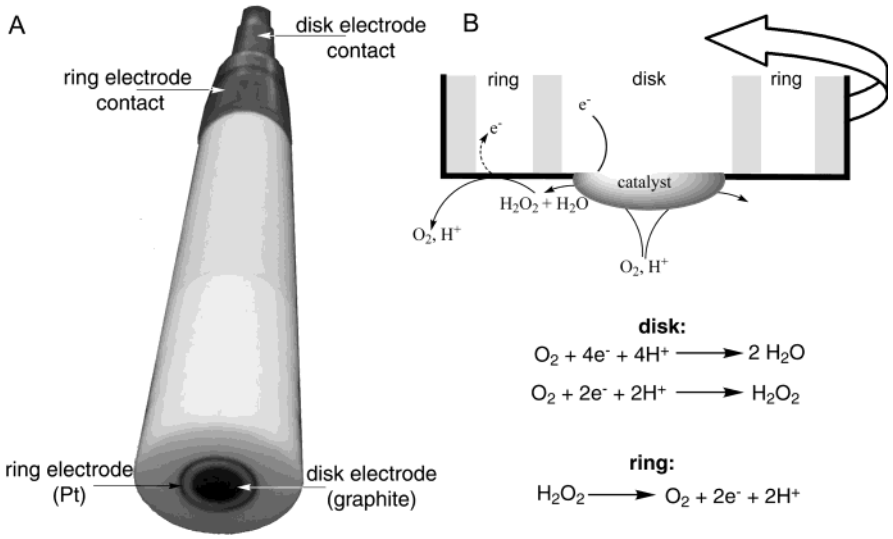

Figure 12. Rotating ring−disk electrode (RRDE). (A) A typical commercially available RRDE. (B) Schematic representation of operating RRDE: rotation of the electrode (block arrow) generates a flow of electrolyte containing the reactants (solid arrows) to the catalyst and sweeps the products of catalysis by the ring electrode. If the catalyst produces H_2O_2 (or O_2^-), a portion of it gets oxidized at the ring, producing current (broken arrow).

available in aqueous solutions often allows detection and/or isolation of intermediates that are too short-lived to be observed when the enzyme reacts with O_2. This impetus is reminiscent of one of the objectives of enzymology in organic solvents.[121,122] The major limitation of this approach as applied to biomimetic studies is that the availability of protons in aqueous media may fundamentally change the dioxygen reactivity of the FeCu core. For example, a negatively charged distal oxygen in a putative ferric−peroxo intermediate can be stabilized by protonation (forming the ferric−hydroperoxo species, which is a proposed intermediate in the CcO catalytic cycle) rather than coordination to Cu (yielding a bridged peroxo derivative, which is commonly observed in biomimetic studies).

The alternative approach, reviewed in detail here, has been to study electrochemical O_2 reduction catalyzed by synthetic heme/Cu analogues. In such studies, biologically relevant conditions of pH, electrochemical potential, and electron flux can be reproduced, and the reactivity can be studied under steady-state turnover. Unfortunately, this method makes the use of spectroscopic techniques to characterize the system during catalysis extremely challenging; so far, electrocatalytic studies have been a kinetic method.

3.2. Methodology of Electrocatalytic Studies of Heme/Cu Analogues

Electrochemistry is particularly fitting for studying catalysis of a redox reaction such as reduction of O_2. Several electrochemical methods are used in biochemistry to assay activity of CcO preparations.[123] The technique that is especially suitable for studying catalytic behavior of biomimetic heme/Cu analogues is rotating ring-disk votammetry,[124] wherein the electrode serves both as a source of electrons and as a catalyst support.[37] A water-insoluble catalyst is deposited, either alone or as a mixture with a matrix compound, on the disk (Figure 12), and the assembly is brought into contact with an aqueous buffered solution. Rotation of the electrode generates a flow of the solution to the electrode, delivering the reactants to the catalyst. The products of the catalysis diffuse (or are hydrodynamically transported) to the ring electrode, set at a potential where H_2O_2 is rapidly oxidized to O_2 (usually between 0.8 and 1 V vs NHE). If the catalyst is less than 100% selective toward $4e^-$ O_2 reduction, i.e., if it reduces a fraction of O_2 only to H_2O_2, this fraction can be quantified by comparing the disk and ring currents. Analysis of the catalytic currents as a function of the electrode rotation frequency (Figure 13) and the substrate concentration allows quantification of both catalytic kinetics and catalytic selectivity (often presented as the average number of electrons by which one O_2 molecule is reduced, n_{av}). In the regime where catalytic currents are directly proportional to both the substrate concentration and the amount of the catalyst at the electrode, the Koutecky−Levich equation provides an adequate general description of the electrode kinetics (Figure 13).[37,125] The slope of a plot of the inverse catalytic currents vs the inverse square-root of the electrode rotation frequency yields n_{av}, and its intercept is proportional to the apparent bimolecular catalytic rate constant.[124] Important mechanistic information is available from an analysis of catalytic currents as a function of the pH.

To maximize the biological relevance of the data collected in such biomimetic electrocatalytic studies, two phenomena must be kept in mind. One is the fact that the kinetics, selectivity, and mechanism of O_2 reduction often depend strongly on the electrochemical potential, with the $4e^-$ pathway becoming increasing more facile at more reducing potentials. At potentials more reducing than those at which heme/Cu terminal oxidases operate in vivo (>50 mV vs NHE), biomimetic catalysis may proceed via intermediates that are not biologically relevant.[37] For example, CcO can couple oxidation of ferrocytochrome *c* ($E°(Fe^{III/II}) \approx 250$ mV) to reduction of O_2, in part

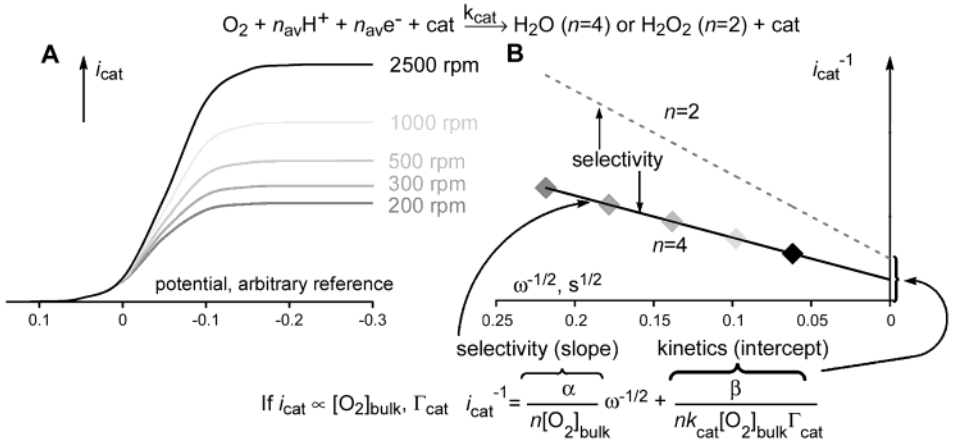

Figure 13. Information output of an electrocatalytic O_2 reduction at a rotating electrode. (A) Typical catalytic current−potential curves (ring currents are omitted) as a function of the electrode rotation frequency (rpm = revolutions per minute). (B) When the turnover frequency is proportional to both O_2 concentration and the amount of the catalyst at the electrode (Γ_{cat}), inverse catalytic currents depend linearly on the inverse square root of the electrode rotation frequency, ω^{-1} (Koutecky−Levich equation). From such plots, the selectivity (n_{av}) and the apparent bimolecular catalytic rate constant (k_{app}) can be derived.

because the stereoelectronic properties of the heme/Cu site allow facile O−O bond heterolysis in a putative ferric−peroxo intermediate. In contrast, a large body of evidence suggests that simple Fe^{III} porphyrins are inefficient in inducing O−O bond heterolysis.[37] While these porphyrins catalyze $4e^-$ reduction of O_2 at relatively reducing potentials (<0 V vs NHE), the catalysis appears to proceed via ferrous−peroxo derivatives (see below), and therefore cannot be considered as an adequate model of O_2 reduction at the heme/Cu site.[37]

The other phenomenon to consider is the relative rates of electron delivery to the catalytic sites and of O_2 reduction. For an Fe−porphyrin catalyst adsorbed on an electrode surface, heterogeneous electron transfer is often rapid, so the turnover frequency is not limited by the rate of electron transport.[37,125] In contrast, as mentioned above, CcO reduces O_2 to the redox level of water (the R → P transformation, Figure 11) at least 10 times faster than it oxidizes a single molecule of ferrocytochrome *c*. Ready availability of electrons can conceivably alter the mechanism of O_2 reduction. Moreover, if the physiological role of a cofactor at the heme/Cu site is mainly electron storage, its presence in a biomimetic catalyst adsorbed on an electrode would have no apparent effect on the kinetics or mechanism of the catalysis, since the ready availability of electrons eliminates the need to *store* electrons within the molecule. Hence, meaningful biomimetic electrolytic studies require one to reproduce the turnover-determining electron transport under which CcO operates in vivo. Applications of rotating ring−disk voltammetry to biomimetic studies of CcO is reviewed in more detail elsewhere.[37]

3.3. General Considerations for the Design of Biomimetic Heme/Cu Analogues for Electrocatalytic Studies

To be amenable to electrocatalytic studies, biomimetic heme/Cu analogues must meet more stringent structural requirements than the models designed solely for studies of stoichiometric O_2 reactivity.[40] Such biomimetic catalysts must not only adequately reproduce the immediate coordination environment of both metals and the Fe···Cu distance, but also retain the structural integrity under catalytic turnover. The latter requirement renders unsuitable "self-assembled" synthetic heme/Cu analogues wherein an iron porphyrin and a Cu complex are held together only by an exogenous bridging ligand, which may be derived from O_2. To overcome these difficulties, several binucleating ligands comprised of a porphyrin moiety and a chelate with at least three coordinating nitrogen atoms have been developed (Figure 14).[67,84,94,126−128] To adequately reproduce the reactivity of the heme/Cu site, these ligands must also contain a heterocyclic moiety (such as imidazole or pyridine) that can serve as a proximal ligand to the Fe. In contrast to solution studies, this proximal ligation cannot be achieved simply by adding an appropriate nitrogenous heterocycle to an aqueous solution in contact with an electrode-confined biomimetic heme/Cu analogue, and therefore has to be built into the ligand.[37] It seems likely that carboxylate residues at the carbon−electrode surface may successfully compete with the dissolved heterocyclic ligand for coordination to Fe. The absence of a covalently attached proximal ligand appears to substantially decrease the rate of catalytic O_2 reduction at physiologically relevant potentials (>50 mV).[37] Because of these structural requirements, all biomimetic heme/Cu analogues used to date in electrocatalytic studies are based on tetrakis(*o*-aminophenyl)-porphyrin, and their synthesis follows well-established protocols (Figure 15).[37,67,84,12]

It could be expected that a properly designed heme/Cu analogue would reproduce not only the structure but also the electronic properties of the enzymatic site, and thus would have potentials of the $Fe^{III/II}$ and $Cu^{II/I}$ couples similar to those observed in CcO, i.e., 220−350 mV[129,130] (the literature values vary; the potentials depend on the redox states of the other cofactors in the enzyme and on the enzyme's protonation state). The importance of reproducing these

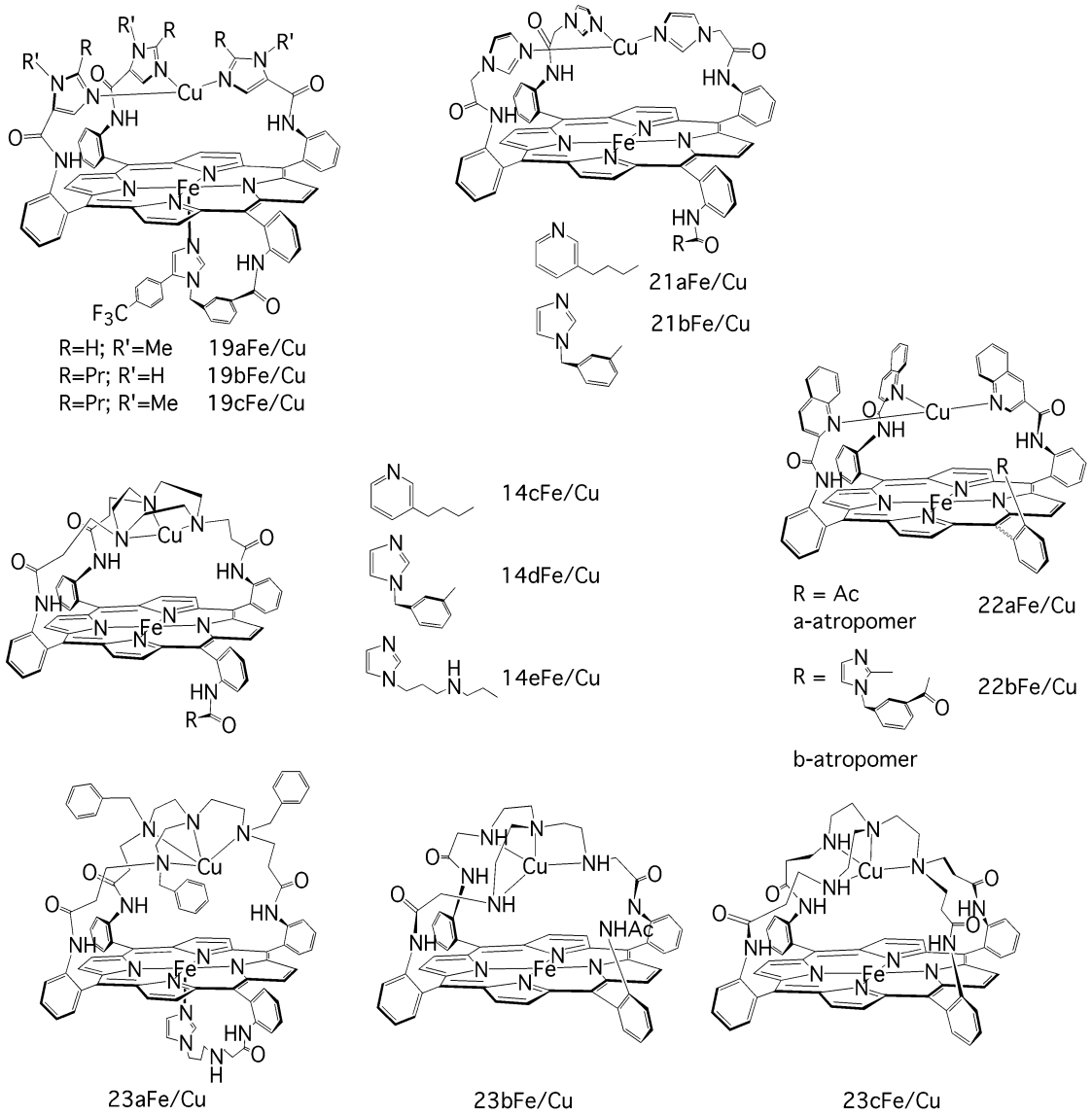

Figure 14. Biomimetic analogues of the heme/Cu site of terminal oxidases whose catalytic properties in electrochemical reduction of O_2 have been reported. Exogenous ligands and counterions are omitted.

potentials is two-fold. First, O_2 affinity of a metal complex correlates with the redox potential of the metal, other things being equal. Second, because neither Fe^{III} nor Cu^{II} binds O_2, the highest electrochemical potential at which catalytic O_2 reduction by a biomimetic heme/Cu analogue can be studied is often determined by the $Fe^{III/II}$ potential. If this potential is more reducing than ~50 mV (vs the NHE), the catalyst may have low if any activity at physiologically relevant potentials, which makes it less useful for biomimetic studies of CcO, as discussed above. This issue of the potentials has been largely ignored in biomimetic studies of CcO, and such potentials are known for only very few heme/Cu analogues. In general, these potentials depend both on the first coordination sphere of the metals and on the polarity of the medium. On the one hand, most heme/Cu analogues are based on the tetraphenylporphyrin motif, which is a substantially weaker σ-base than protoporphyrin and makes the $Fe^{III/II}$ potential more reducing.[131] On the other hand, synthetic heme/Cu analogues are studied electrochemically in a medium substantially more polar than the protein matrix, which favors the ferric state. The issue of the polarity of the medium was addressed explicitly in two recent papers.[133,134] The interplay of these and possibly other phenomena affects the biological relevance of the chemistry observed for synthetic heme/Cu analogues.

3.4. Electrocatalytic O_2 Reduction by Simple Fe Porphyrins

Understanding the structure/reactivity relationship at the heme/Cu site of terminal oxidases using the technique of biomimetic electrocatalytic O_2 reduction first requires an understanding of the properties of simple Fe porphyrins, such as Fe(TPP), in such a reaction.[132] This simple truth, however, has until recently been largely ignored by the CcO biomimetic community. Electrochemical reduction of O_2 and occasionally of H_2O_2 by simple Fe porphyrins immobilized on a graphite electrode has been studied fairly extensively over the past 25 years. While there is substantial disagreement in the literature regarding the quantitative aspects of this reactivity (Table

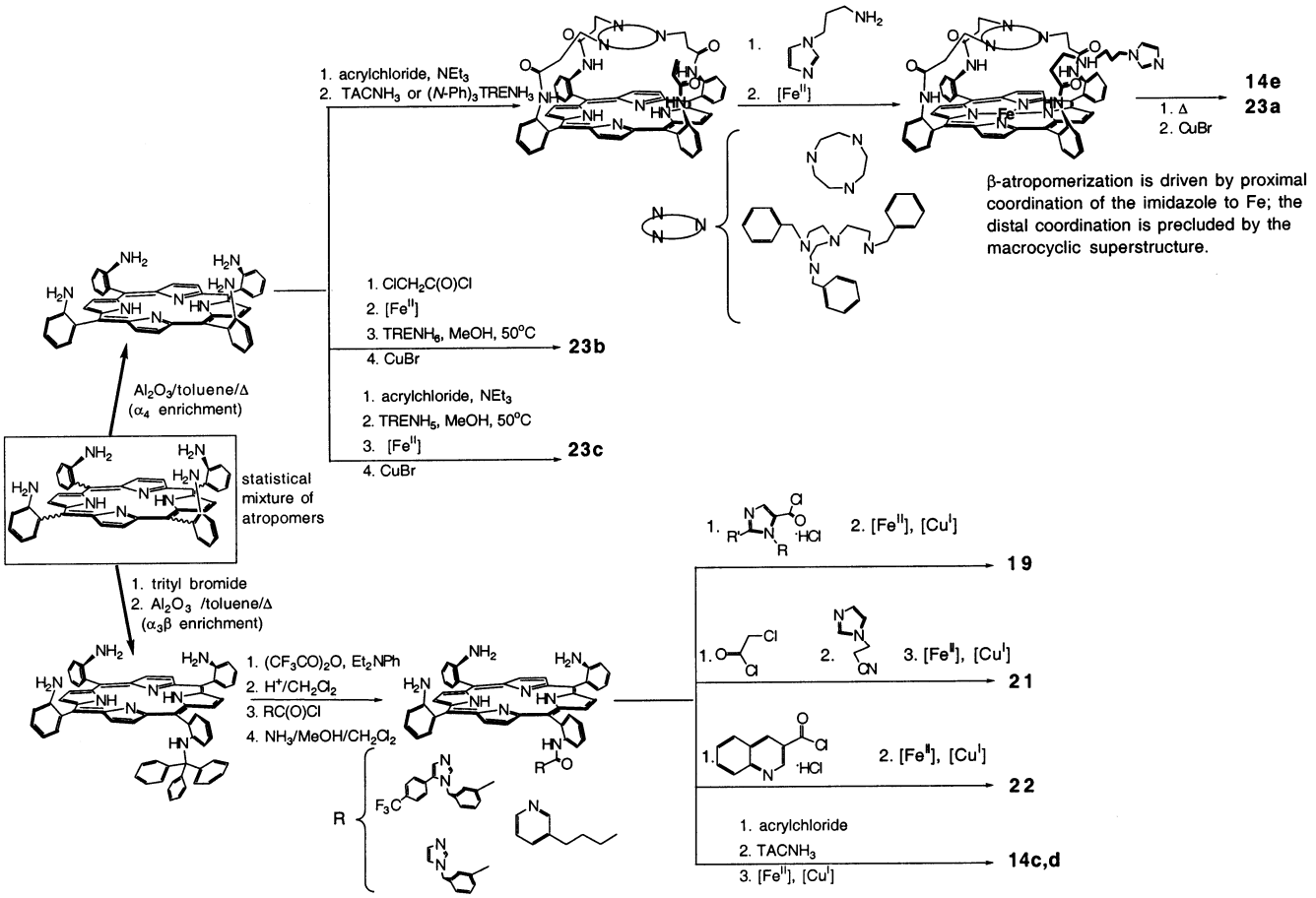

Figure 15. Typical syntheses of the compounds shown in Figure 14. All compounds are based on tetra(*o*-aminophenyl)-porphyrin and utilize either an α_4 or $\alpha_3\beta$ atropomer. [Fe^{II}] is usually $FeBr_2$ in 2,6-lutidine, acetic acid, or boiling methanol as solvent; [Cu^I] is usually a Cu^I salt with a noncoordinated anion in acetonitrile.

5), qualitatively, simple Fe porphyrins behave similarly (L'Her and co-workers recently presented results that contradict this body of prior work, proposing that the porphyrin−porphyrin aggregation of sterically unencumbered Fe porphyrins in the solid state is an unrecognized phenomenon that affects their electrocatalytic properties.[128a]):

1. Electrocatalytic reduction of O_2 or of H_2O_2 starts at potentials close to that of the $Fe^{III/II}$ couple (measured under anaerobic conditions).

2. The pH dependence of the catalytic half-wave potentials ($E_{1/2}$) and the $Fe^{III/II}$ potentials in the absence of O_2 is identical: either 60 or 0 mV/pH, depending on the electrolyte acidity (Table 5). This suggests that, in the potential-dependent regime of catalysis, the turnover frequency depends directly on the surface concentration of ferrous catalyst and the turnover-determining step does not involve an electron transfer (e.g., it is O_2 binding).

3. The redox stoichiometry of O_2 electroreduction (n_{av}) by films of Fe porphyrins is not affected significantly by the pH (1−14 in the few studied cases).

4. The turnover frequency of simple *ferric* porphyrins in H_2O_2 reduction is below the detection limit of the electrocatalytic experiment, whereas the rate of electrocatalytic H_2O_2 reduction by *ferrous* analogues is comparable to that of O_2 reduction.

5. The catalysis likely proceeds via peroxo-type intermediates such as $[(por)Fe^{III}(O_2H_x)]^{(x-1)}$ and/or

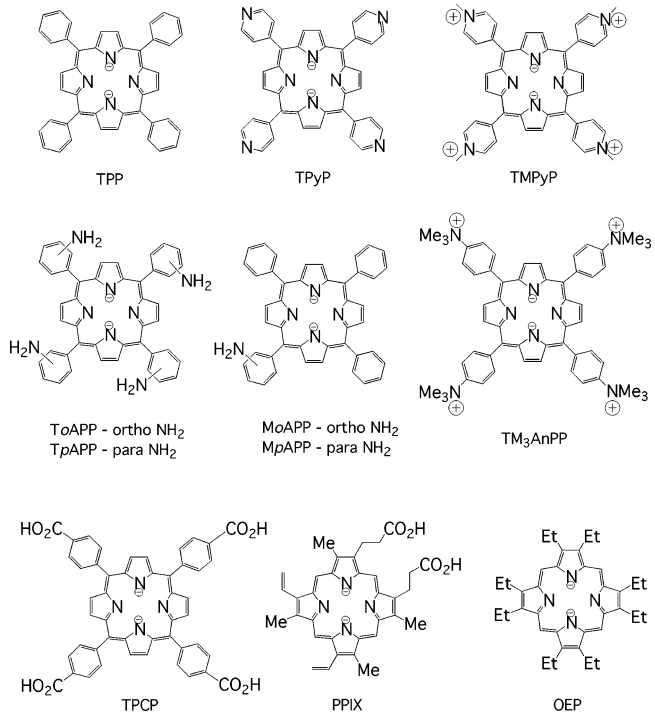

Figure 16. Chemical structures and trivial names of simple Fe porphyrins whose electrocatalytic properties in reduction of O_2 and H_2O_2 have been reported.

$[(por)Fe^{II}(O_2H_x)]^{(x-2)}$ ($x = 1, 2$). The low reactivity of Fe^{III}−porphyrins toward H_2O_2 is probably due both

Table 5. Summary of the Electrocatalytic Properties of Simple Fe Porphyrins Immobilized on an Electrode [See Figure 16 for the Relevant Chemical Structures; All Potentials vs the Normal Hydrogen Electrode (NHE)]

catalyst (Figure 16)	$E(Fe^{III/II})$[a]	$E_{1/2}$ (RDE), V[b]		selectivity (n_{av})[c]		pH dependence (pH range)	$E_{1/2}$, H_2O_2	experimental conditions	ref
		pH 0−2	pH 7	at $E_{1/2}$	at plateau				
(TPP)Fe	0	0.35, 0.2[d]			3.7 KL			glassy carbon, O_2-saturated 0.05 M H_2SO_4, 100 rpm	135
(TPP)Fe[e]	0.5, 0.1	0.35−0.2	0.1	n.r.	4 KL	60 mV/pH (pH > 3), 0 mV/pH (pH < 3)		edge-plane graphite, O_2-saturated electrolyte buffered at various pH, 100 rpm	136
(TPP)Fe[g]	0.1	0.35, 0.2[d]			3.7 KL, 4 i_r/i_d		0.1	pyrolytic graphite, O_2-saturated 0.1 M $HClO_4$, 100 rpm	137
(TPP)Fe[f]	n.r.	0		*f*	3.2 KL			film prepared from (TPP)FeCl: glassy-carbon, reported as O_2-saturated 0.5 M $HClO_4$ but the shown catalytic currents are ∼60−70% of the diffusion-limited current at $[O_2] = 1.3$ mM	138
(TPP)Fe	0.06	0		*f*	3.7 KL		inert	film prepared from $[(TPP)Fe]_2$-(μ-O), other parameters are the same as above	138
(TPyP)Fe	0.2	0.35		3.7	3 KL		0.2	pyrolytic graphite; O_2-saturated 0.1 M $HClO_4$ or 0.2 M $NaClO_4$ + NaOH to pH 12; 100 rpm	137
(TMPyP)Fe	0.5	0.25			4 KL	0 mV/pH (pH < 7), 60 mV/pH (pH > 7)	0.2	glassy carbon, O_2-saturated 0.1 M H_2SO_4; buffered solutions for pH dependence; catalyst in solution but the observed properties may be those of electrode-adsorbed catalyst	136, 139
(T*p*APP)Fe	0.1	0.2		3.5	4 KL			glassy carbon, O_2-saturated 0.05 M H_2SO_4, 100 rpm	135
(T*o*APP)Fe	0.1	0.2		3.5	4 KL			glassy carbon, O_2-saturated 0.05 M H_2SO_4, 100 rpm	135
(T*o*APP)Fe	0.2	0.3	0	*g*	4 KL, i_r/i_d	65 mV/pH (2−7), 0 mV/pH (1, >7)		glassy carbon, air-saturated 0.05 M H_2SO_4 (buffered electrolyte for pH dependence), 100 rpm	140
(M*p*APP)Fe	0.1	0.2		3	3.9 KL			glassy carbon, O_2-saturated 0.05 M H_2SO_4, 100 rpm	135
(M*o*APP)Fe	0.1	0.2		3	3.9 KL			glassy carbon, O_2-saturated 0.05 M H_2SO_4, 100 rpm	135
(TM_3AnPP)-Fe	0	0.2	0	3.4 (pH 8)	3.8 i_r/i_d (pH 8)	55 mV/pH (1−4, 6−8), 0 mV/pH (0−1, 4−6, 8−10)		glassy carbon, air-saturated pH 2 electrolyte; 400 rpm	141
(TPCP)Fe	0.3	0.1			>2	55 mV/pH (pH 0−2)	0.1	stationary glassy carbon, air-saturated 0.05 M H_2SO_4	142
(PPIX)Fe	0.1	0.2	0	3	3.8 KL	60 mV/pH (2.5−5.5, >8.5), 0 mV/pH (1−, 2.5, 5.5−8.5)[h]	0.1	pyrolytic graphite, O_2-saturated 0.1 M $HClO_4$ (buffered electrolytes for pH dependence), 100 rpm	137
(PPIX)Fe	0						0.2	covalently attached to Au; air-saturated pH 7 buffered	
(OEP)Fe	n.r.	0.2		*f*	3.5 KL			electrolyte film prepared from (OEP)FeCl; glassy carbon, reported as O_2-saturated 0.5 M $HClO_4$ but the catalytic currents shown are ∼60−70% of the diffusion-limited current at $[O_2] = 1.3$ mM	138
(OEP)Fe	n.r.	0.2		*f*	3.8 KL			film prepared from $[(OEP)Fe]_2$-(μ-O), other parameters are the same as above	138

[a] In the absence of a substrate; n.r., not reported. [b] The half-wave potential of the catalytic wave for O_2 reduction at a rotating disk electrode. This value depends on the electrode rotation rate, bulk O_2 concentration, pH, and in many cases the scan rate, the amount of the adsorbed catalyst, and the nature of the supporting electrolyte. [c] The apparent redox stoichiometry of O_2 reduction. We have calculated the n_{av} values at $E_{1/2}$ from the presented RRDE LSVs using the collection efficiencies reported by the authors or estimated from an RRDE trace for O_2 reduction on bare electrode. The method by which n_{av} was estimated: KL, the Koutecky−Levich plot (Figure 13B); i_r/i_d, the ring-to-disk currents ratio when the collection efficiency is reported or could be estimated. [d] Two waves (see Figure 17A). [e] The adsorbed catalyst yields two surface redox waves in the absence of a substrate, presumably corresponding to two different forms; only the form with the more positive redox potential was reported to be catalytically active. The authors do not mention the presence of two catalytic waves in O_2 reduction; the $E_{1/2}$ was reported to be dependent on the surface concentration of the catalysts; the range of the observed $E_{1/2}$ values is given.[136] [f] No data are provided to determine the experimental collection efficiency of the RRDE toward H_2O_2, and the ring current appears to be potential-independent (Figure 17C); a single catalytic wave is observed in linear sweep voltammograms of the (TPP)Fe catalyst. [g] The experimental collection efficiency is not reported, and the i_r-E profile is similar to that in Figure 17A. [h] The pH dependence of the $Fe^{III/II}$ potential in the absence of a substrate is shown; the $E_{1/2}$ vs pH dependence appears to be similar.

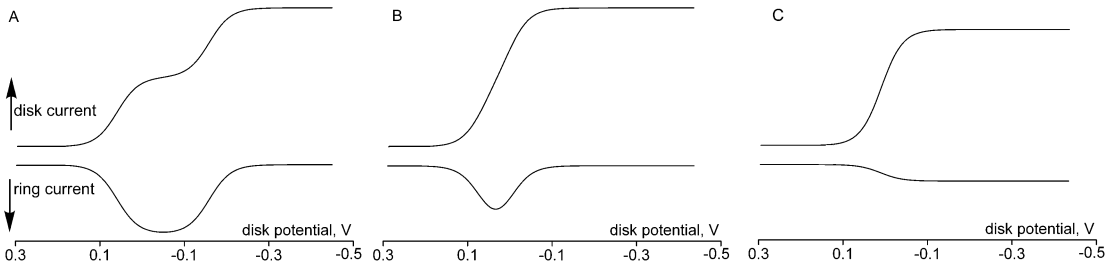

Figure 17. Typical rotating ring−disk voltammograms for O_2 reduction by simple Fe porphyrins immobilized on a graphite electrode. Simulated traces based on data in ref 137 for (A) Fe(TPP), (B) Fe(PPIX), and (C) Fe(TPyP) in a pH 0 electrolyte. Qualitatively similar voltammograms are observed at other pH values.

to the slower ligand exchange at a ferric vs a ferrous center and to less facile O−O bond heterolysis in ferric−peroxo adducts (as it generates higher-energy intermediates, e.g., ferryl-porphyrin π-cation radical).

6. The selectivity of O_2 reduction by multilayer films of many electrode-confined Fe porphyrins is potential-dependent (three major types of the $i-E$ profiles observed in O_2 reduction are shown in Figure 17), but the origin of such behavior is poorly studied. The 4e O_2 reduction at the plateau is believed to proceed via a two-step mechanism, whereby O_2 reduction by individual Fe porphyrin molecules generates a substantial H_2O_2 flux, but, under the condition of high catalyst-to-substrate ratio, the released H_2O_2 is reduced to H_2O (or disproportionated) by neighboring catalyst molecules before it diffuses out of the film and is detected. The potential-dependent selectivity of a catalytic film indicates a kinetic competition between a potential-independent source of free H_2O_2 and a potential-dependent sink (or vice versa). A decreasing H_2O_2 flux at more reducing potentials (Figure 17A,B) is commonly ascribed to an increased fraction of the more-reactive-toward-H_2O_2 ferrous porphyrin.[136] This explanation assumes the presence of a potential-dependent *sink* (higher fraction of the more reactive Fe^{II} species), but the possibility of a potential-dependent *source* as the origin of the selectivity profile cannot at present be ruled out, and it may be more consistent with the known chemistry of Fe porphyrins. The catalytic selectivity may increase at potentials where the ferrous−peroxo intermediate becomes electrochemically favorable over the ferric−peroxo analogue. Because O−O bond cleavage in the former is less facile than in the latter, decomposition of $[(por)Fe^{II}(O_2H_x)]^{(x-2)}$ intermediates ($x = 1, 2$) may preferentially proceed via O−O bond cleavage as opposed to peroxide dissociation in the case of $[(por)Fe^{III}(O_2H_x)]^{(x-1)}$ analogues. Whether 4e O_2 reduction by simple Fe porphyrins proceeds by the "two-step" mechanism via free H_2O_2 or without the intermediacy of free H_2O_2 via ferrous−peroxo intermediates, such 4e activity is biologically irrelevant, as intermediates of neither type are accessible or existent in heme enzymes.

7. In catalytic O_2 reduction, Fe porphyrins manifest low stability, but the decomposition pathway(s) are not established. Oxidative degradation of Fe porphyrin complexes without meso substituents (e.g., OEP and PPIX, Figure 16) can proceed via a nucleophilic attack of the Fe-bound superoxo moiety on the meso carbon (heme oxygenase mechanism),[143] and a direct attack of H_2O_2 on the meso carbon may also be possible.[144] In contrast, the oxidation mechanism of meso-substituted porphyrins (which are usually thought to be more resistant to bleaching) is not known. Bimolecular oxygenation of the macrocycle by oxoferryl derivatives appears probable in homogeneous catalytic systems,[145] but such a mechanism is not easily accessible for an adsorbed Fe porphyrin. Although it is generally assumed that H_2O_2 is primarily responsible for catalyst degradation during O_2 reduction, the most plausible candidate is $^{\bullet}OH$, which is substantially more reactive, thermodynamically ($E° \approx 2.8$ V) and kinetically, than O_2^-/HO_2 or H_2O_2.[146−148] Indeed, $^{\bullet}OH$-mediated degradation explains the fact that purely 2e catalysts (simple Co porphyrins) display substantially higher stability (turnover numbers) in electrocatalytic O_2 reduction than many structurally related metalloporphyrins, which catalyze the 4e pathway. Thus, the stability of an electrocatalyst during O_2 reduction may provide a qualitative measure of its selectivity toward heterolysis vs homolysis of the O−O bond.

8. The very limited stability of Fe catalysts in O_2 reduction may also explain the fact that the apparent selectivity of O_2 reduction at an Fe−porphyrin-modified electrode correlates positively with the amount of the deposited metalloporphyrin. As a smaller fraction of "thicker" catalytic films decomposes during a catalytic run, such films manifest higher apparent selectivities, assuming that the intact catalyst is more selective than a partly decomposed analogue.

Studies of electrocatalytic O_2 reduction by simple Fe porphyrins suggest that such species, when adsorbed on the electrode, catalyze selective 4e O_2 reduction at sufficiently reducing potentials (the effect of electron availability on the selectivity of Fe porphyrins has recently been studied experimentally[149]). This 4e O_2 reduction, however, is not biologically relevant, as it appears to proceed via intermediates that are inaccessible or nonexistent in enzymatic heme catalysis. The low stability of most Fe porphyrins in electrocatalytic O_2 reduction, even in the regime when apparent 4e O_2 reduction is observed, is likely due to production of hydroxyl radicals, revealing the contribution of Fenton chemistry to the catalysis. This illustrates that the capacity to effect 4e O_2 reduction at an arbitrary electrochemical potential and for an arbitrary small number of turnovers is not an indication that a metalloporphy-

Table 6. Electrocatalytic Properties toward O_2 Reduction of the Functional Heme/Cu Site Analogues [See Figure 14 for the Relevant Chemical Structures; All Potentials vs the Normal Hydrogen Electrode (NHE)]

catalyst (Figure 14)	E_{cat}, V [a]	$E_{1/2}(O_2)$, V at pH 7 [b]	selectivity (n_{av}) [c] at $E_{1/2}$	selectivity (n_{av}) [c] at plateau	ref
19Fe/Cu [d]	0.1	0.2	~4	4	125
19Fe [d]	0.1	0.2	>3.7−3.8	4	125
21a Fe/Cu	n.r.	0.2 [e]	n.r.	4 [f]	126
21b Fe/Cu	~0.25	0.15	n.r.	4 [f]	126
22a Fe/Cu	n.r.	0	2.5−3.5	3.4 i_{lim} (3.8 i_r/i_d)	152
22a Fe	n.r.	0	2.2−3.4	3.5 i_{lim} (3.9 i_r/i_d)	152
22b Fe/Cu	n.r.	0.1	<3.1	3.5 i_{lim}	152
22b Fe	n.r.	n.m.		3.6 i_{lim}	152
23b Fe/Cu	n.r.	0	<2.6	2.7 i_r/i_d	151
23b Fe	n.r.	0	<3.8	4 i_r/i_d	151
23c Fe/Cu	n.r.	0.05	2.5−3	2.8 i_{lim} (3.2 i_r/i_d)	151
23c Fe	n.r.	0	3.7−3.8	4 i_r/i_d	151
23a Fe/Cu	~0.15 (Fe); ~ −0.2 (Cu) [g]	0.15 [f]	n.r.	4−3.6 [h] KL	44, 153
14c Fe/Cu	n.r.	0.15	n.r.	3.9, KL	94
14d Fe/Cu	n.r.	0.2	n.r.	3.9 KL	94
14e Fe/Cu	~0.1 (Fe); ~0.5 (Cu) [g]	0.15	n.r.	2−3.1 [h]	44, 153
14e Co/Cu	~0.7 (Co); ~0.3 (Cu)	0.25	4	3.9 KL	154

[a] The redox couple ($Fe^{III/II}/Cu^{II/I}$ or $Fe^{III}Cu^{II}/Fe^{II}Cu^{I}$) for the graphite-adsorbed catalyst in the absence of a substrate; n.r., not reported. [b] The half-wave potential of the catalytic wave for O_2 reduction by rotating disk voltammetry. This value depends on the electrode rotation rate, bulk O_2 concentration, pH, and in many cases the scan rate, the amount of the adsorbed catalyst, and the nature of the supporting electrolyte; n.m., not meaningful (no defined wave). [c] The apparent redox stoichiometry of O_2 reduction. We have calculated the n_{av} values at $E_{1/2}$ from the linear sweep voltammograms presented by the authors using the collection efficiencies reported by the authors or estimated from rotating ring−disk voltammogram of O_2 reduction on a bare graphite electrode. The method whereby n_{av} was estimated: KL, the Koutecky−Levich plot (Figure 13B); i_r/i_d, the ring-to-disk currents ratio when the collection efficiency is reported or could be estimated; i_{lim}, comparison of the limiting current yielded by the catalyst with that given by the standard with a known n_{av} under the identical experimental conditions. The higher n_{av} values estimated from the i_r/i_d ratio for several entries illustrate that the reported collection efficiencies are significantly overestimated. [d] The imidazole substitution pattern of the distal superstructure has only a minor effect on the electrochemical behavior. [e] The numbers were extracted from the voltammograms given in the Supporting Information. [f] "No detectable peroxide leakage"; neither rotating ring−disk voltammograms nor i_r/i_d values are presented, and the experimental collection efficiency is not specified. [g] The peaks labeled as $Cu^{II/I}$ are poorly defined and only quasi-reversible; these peaks may not correspond to the $Cu^{II/I}$ couple. [h] The first number refers to the originally reported selectivity; the second *n* value was reported later.

rin adequately reproduces the catalytic mechanism of the heme/Cu site in CcO, and thus can be considered a "functional" analogue. Failure to take into account this fact leads to unreasonable conclusions regarding the structure/reactivity relationship at the heme/Cu site. A minimum requirement for an electrocatalyst to be a functional heme/Cu analogue is its capacity to effect largely 4e O_2 reduction at *physiologically relevant potentials* (e.g., those of cytochrome *c* and ubiquinol) without production of free $^{\bullet}OH$.

3.5. Biomimetic Electrocatalytic Studies Prior to 2000

Until about the year 2000, the main objective of electrocatalytic studies with biomimetic heme/Cu analogues was to design catalysts with maximum selectivity toward 4e O_2 reduction, regardless of the electrochemical potential.[37] This objective, however, is problematic. First, only catalysis at physiologically relevant potentials (>50 mV) is likely to be representative of the mechanism of O_2 reduction by heme/Cu terminal oxidases. Second, it was shown as early as the 1980s by Anson[136,137] and later by others[135,138,141,142,150] that even simple Fe porphyrins, when adsorbed on an electrode, catalyze selective O_2 reduction at potentials <0 V vs NHE (see above). Because of this, further improvement of the catalytic selectivities through structural elaboration of the distal/proximal environments seemed unlikely to yield substantially higher selectivity under similar conditions. This was confirmed by L'Her and coworkers (Table 6).[128,151] Interestingly, however, incorporation of Cu into some of these heme/Cu analogues appears to *lower* selectivities! For example, Boitrel's and L'Her's catalysts (derivatives of **23b**, Figure 14)[152] demonstrate respectable selectivity (n_{av} between 3.7 and 4, depending on the potential) in the Fe-only form, whereas the FeCu analogues catalyze O_2 reduction largely to H_2O_2 (Table 6). The authors hypothesized that this startling result arises because the "copper center does not interfere with the O_2 molecule bound to Fe" or the "copper ion...is no longer coordinated". It appears more likely, however, that the lower apparent selectivity of the FeCu derivatives may arise from faster degradation of the bimetallic catalyst relative to the monometallic analogue. Such rapid degradation of an immobilized Fe porphyrin can conceivably be mediated only by hydroxyl radicals, which seems to suggest that Cu coordinated to these particular ligands *facilitates* O−O bond homolysis either in Fe-bound peroxo species or in free H_2O_2, which is generated as a byproduct of O_2 reduction.[132] Other examples of heme/Cu analogues with remarkably low selectivities toward 4e$^-$ O_2 reduction in the bimetallic form have been reported.[153] The reader is referred to a recent review of electrocatalytic studies of biomimetic CcO analogues and simple Fe porphyrins covering the literature through the year 2000 for a detailed discussion of these topics.[37]

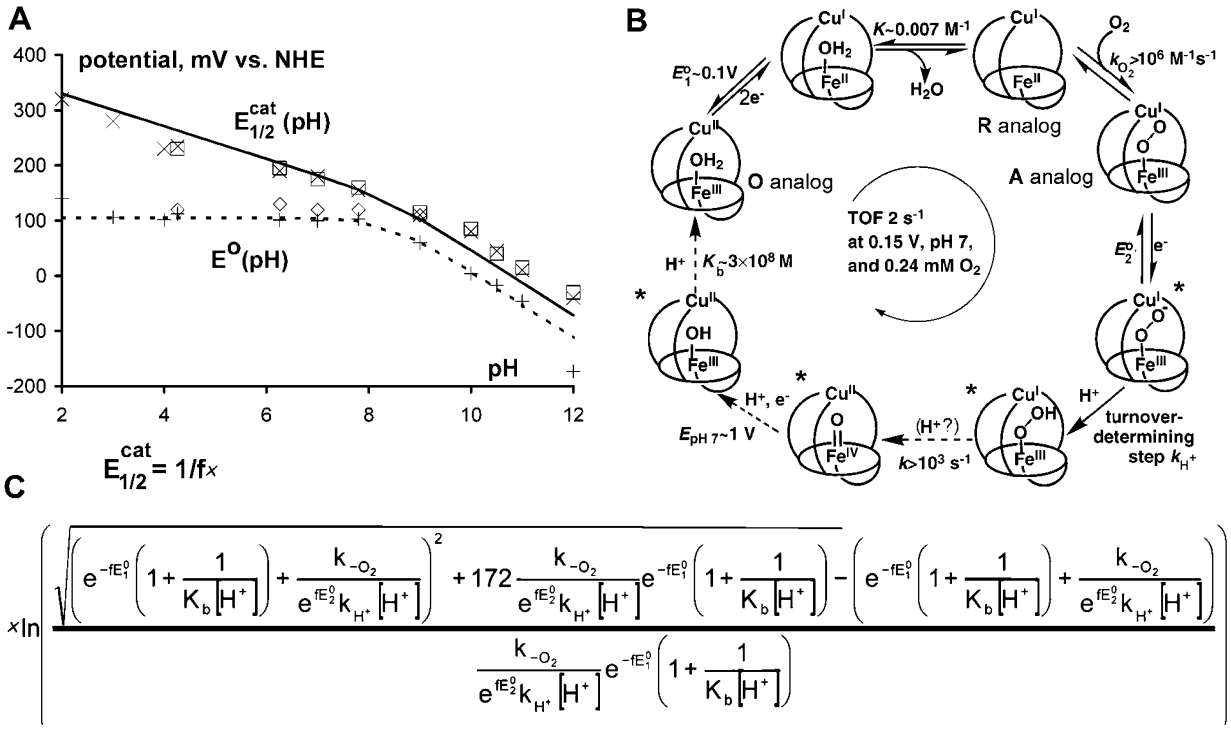

Figure 18. Catalytic mechanism of O_2 reduction by **19** (Figure 14). (A) The pH dependence of the standard potentials in the absence of O_2, $E°$ (+, $Fe^{III/II}$ potential of the Cu-free catalyst; ◇, $Fe^{III}Cu^{II}/Fe^{II}Cu^{I}$ potential of the FeCu catalyst) and of the catalytic half-wave potentials, $E°_{1/2}$ (×, the Cu-free catalyst; □, the FeCu catalyst). Note that the dependences are identical for both the Cu-free and FeCu catalysts. The least-squares fit (LSF) of the $E°$ vs pH data (A, broken line) indicates a water molecule (with $pK_a = 8.4$) as an exogenous sixth ligand at the Fe. The $E°_{1/2}$ vs pH data reveal two reversible electron-transfer steps and a protonation as components of the turnover-determining part of the catalytic cycle. The mechanism in B is most consistent with these data (analogues of compounds O, R, and A of the CcO cycle, Figure 11, are indicated); steps indicated by broken arrows are kinetically "invisible" at pH < 9 and are inferred on the basis of the stoichiometry of the cycle. Thermodynamics and/or kinetics of individual steps in this mechanism were determined independently.[125] On the basis of these data, a rate law was derived (C) which fits well the experimental data (A, solid line) using a single adjustable parameter, ($k_{-O_2}\, e^{-fE°_2}/k_{H^+}$). The structures of intermediates indicated with asterisks are unknown; the other intermediates were prepared independently and characterized spectroscopically. Note that the oxygenated catalyst is a ferriheme−superoxide/Cu^{I} isomer (compound A analogue), not the Fe^{III}−O−O−Cu^{II} isomer usually observed in biomimetic CcO analogues.[99]

3.6. Role(s) of Cu_B Based on Biomimetic Electrocatalytic Studies

A series of papers published in 2002−2003 describe the most informative study to date addressing the possible roles of Cu_B in steady-state O_2 reduction by CcO using the biomimetic approach.[84,99,125,133,155,156] This study employed synthetic porphyrins (**19**, Figure 14) that most closely reproduce the stereoelectronic environment of the Fe−Cu core in the heme/Cu site among any complexes known. The authors provided evidence that their complexes reproduce the reactivity of the heme/Cu site with O_2 and H_2O_2 under both catalytic and stoichiometric conditions, specifically:

1. The $Fe^{III/II}$ and $Cu^{II/I}$ potentials are very similar (Table 6), as they are in CcO, although the oxidized states are stabilized relative to those in CcO, probably as a result of the more polar environment in which the complexes were studied.[133]

2. The complexes catalyze O_2 reduction at physiologically relevant potentials (>50 mV) with respectable selectivity toward the $4e^-$ pathway (>96%, $n_{av} > 3.8$) and retain this selectivity for at least 10 000 turnovers.[125] The latter was used to conclude that the catalysts do not induce significant O−O bond homolysis, which produces highly destructive hydroxyl radicals. Because of the high reactivity of •OH, they do not reach the ring of the rotating ring−disk electrode, but rapidly bleach the catalyst.

3. By analyzing the effect of the pH on catalytic currents in the regime where the catalytic currents were proportional to both O_2 concentration and the amount of deposited catalyst, the authors derived a kinetic mechanism for the catalytic cycle (Figure 18).[125] They showed that a formally ferric−hydroperoxo intermediate is generated more slowly than it is reduced further, which explains the high selectivity of these catalysts toward 4e O_2 reduction. A common source of H_2O_2 in metalloporphyrin-catalyzed O_2 reduction appears to be hydrolysis of the ferric−hydroperoxo intermediate.[37] When this intermediate is generated more slowly than it is being consumed, its steady-state concentration is very low, which minimizes the amount of H_2O_2 that can be released into the medium. A similar sequence of steps was proposed for the conversion of compound A to compound P in CcO (Figure 11).[120]

4. The maximum turnover rates of O_2 reduction, as well as of H_2O_2 reduction catalyzed by the reduced ($Fe^{II}Cu^{I}$) and oxidized ($Fe^{III}Cu^{II}$) forms of **19**, were found to be comparable to the rates reported for CcO.[125] These are the only synthetic porphyrins that, in the oxidized form, catalyze H_2O_2 reduction fast

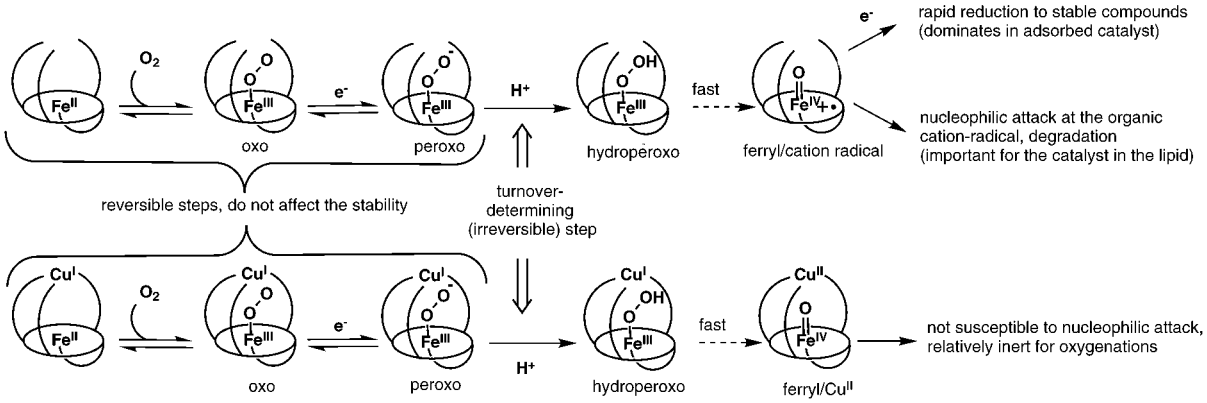

Figure 19. A plausible mechanism for rapid degradation of the Cu-free CcO analogue **19**Fe in the regime of slow electron flux, as opposed to the high stability of **19**Fe/Cu under these conditions and the high stability of **19**Fe in O_2 reduction under an excess of electrons. It is assumed that the catalytic mechanism (Figure 18) is the same in both regimes of electron flux. O−O bond heterolysis in the formally ferric−hydroperoxo intermediate of the Cu-free catalyst results in 1e oxidation of the organic ligand. The resulting cation radical is susceptible to nucleophilic attack by water, buffer, etc. unless it is reduced rapidly. Such rapid reduction is possible when electrons are in excess (i.e., in the electrode-adsorbed catalyst), but not when they arrive only slowly (for the lipid-dispersed catalyst). In contrast, O−O bond heterolysis in **19**Fe/Cu does not generate an organic radical as Cu^I is oxidized, resulting in greater stability of **19**Fe/Cu.

enough to be observed electrochemically. These kinetic data suggest that the stereoelectronic properties of **19** are such that the catalysts, as CcO, efficiently heterolyze the peroxo O−O bond in the oxidized Fe^{III}-Cu^{II} state.

5. Oxygenation of the reduced FeCu complex under nonprotic conditions results in a relatively stable ferric-superoxo/Cu^I adduct,[99] which is analogous to compound A of CcO (Figure 11). In all other systems, the μ-peroxo derivative is the favored product: although transient formation of $Fe^{III}-(O_2^{-})\cdots Cu^I$ species can be sometimes detected, it invariably reverts to the $Fe^{III}-(O_2^{2-})-Cu^{II}$ form.[37,40]

To understand the effect(s) of Cu on the O_2 reduction catalysis by these complexes, the authors compared the electrocatalytic behavior of the FeCu and Cu-free forms of biomimetic analogues **19** under both rapid (non-turnover-determining)[125] and slow (turnover-determining)[155] electron transport. It was assumed that if Cu lowers the activation barrier for O−O bond reduction, then the FeCu complex would be a more active catalyst in both regimes of electron transport. However, if the difference in the activities of the FeCu and Cu-free forms were to be observed only in the (biologically relevant) regime of slow electron transport, then Cu serves mainly as an electron storage site, which provides an electron to the heme but otherwise does not participate in the catalysis.

The regime of rapid electron transport was implemented by adsorbing the pure catalysts at the electrode surface,[125] whereas incorporating the catalysts at a low molar fraction (<3%) into a lipid membrane at the electrode surface reproduced a slow electron flux.[155] In the lipid, the catalyst is present as isolated mobile sites, so electron transfer can occur only when a molecule diffuses to the electrode surface or encounters another molecule of the correct redox state. It was established that cyclic voltammetric (CV) peak currents for reduction (oxidation) of the *adsorbed* catalyst in the absence of a substrate are proportional to the scan rate,[133,156] and that the catalytic currents generated by an adsorbed catalyst are proportional to the O_2 concentration and depend on the electrode rotation frequency according to the Koutecky−Levich equation (Figure 13).[156] In contrast, *a catalyst in the lipid* manifested CV currents under N_2 that are proportional to the square-root of the scan rate, and generated catalytic currents at physiologically relevant potentials that are independent of the O_2 concentration or the electrode rotation frequency.[155]

When electron transport is fast, the turnover frequency, turnover numbers, and mechanisms of both O_2 and H_2O_2 reduction by **19** are largely independent of the presence of Cu, although the selectivity of the FeCu catalyst toward 4e O_2 reduction is notably higher (see below).[125] In the lipid, however, only **19**FeCu is active in O_2 reduction, whereas the Cu-free derivatives rapidly lose their activity. Such lower stability of the Cu-free forms may arise from oxidation of the organic ligand during reduction of O_2, followed by nucleophilic attack of the solvent, etc. on the resulting cation radical (Figure 19). Importantly, the lack of catalytic activity of the Cu-free analogues of the heme/Cu site in the regime of slow electron transport is reminiscent of the results with the Cu_B-free mutants of heme/Cu terminal oxidases.[113,115,157] This suggests that in both cases the absence of the catalytic activity may not be due to the intrinsic inability of the heme alone to reduce O_2 to H_2O, but rather due to rapid decomposition of the catalytic site.

On the basis of these results, it was hypothesized that O_2 reduction at the Cu-free forms of **19** proceeds via a mechanism and with activation parameters similar to those of **19**Fe/Cu. Therefore, it appears that in CcO, Cu_B may serve mainly as an electron storage site, which allows decoupling of the O_2 reduction rate from the rate of electron delivery from ferrocytochrome *c*, but Cu_B does not provide a reaction pathway that is lower in activation energy that would be available for the heme alone.

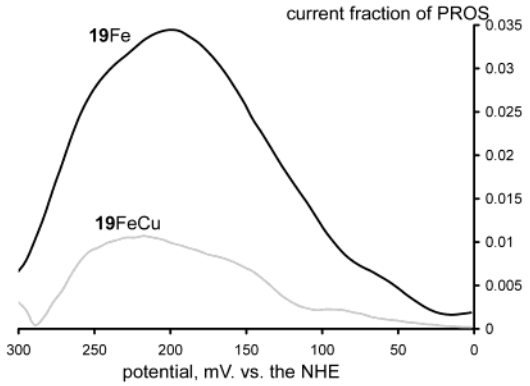

Figure 20. Fractions of catalytic currents consumed by **19**Fe and **19**FeCu that are released as partially reduced oxygen species (PROS, H_2O_2 or O_2^-) under rapid electron flux as a function of the electrochemical potential.[125]

The role of Cu_B as a "conduit" of electrons in CcO was suggested from studies using a myoglobin containing an engineered heme/Cu_B site.[43]

To understand why **19**Fe/Cu is significantly more selective toward 4e O_2 reduction relative to the Cu-free analogues (Figure 20) in the regime where both forms of the catalyst have similar catalytic kinetics and mechanism, catalytic O_2 reduction was examined in the presence of selective superoxide reductants (e.g., trolox and *N*-(mercaptopropionyl)-glycine, MPG).[125] The use of superoxide dismutase, however, was precluded by the experimental setup. In rotating ring−disk voltammetry, the ring current by itself does not provide information about the contributions of O_2^- and H_2O_2 to the partially reduced oxygen flux generated by the catalyst. However, in the presence of superoxide reductants, free O_2^- is rapidly reduced to H_2O_2. This reduction increases the ring current (because it takes twice as much current to oxidize H_2O_2 to O_2 than O_2^-), without contributing to the disk current (because the chosen superoxide reductants are not electroactive at physiologically relevant potentials). Hence, an apparent increase in the ring-to-disk current ratio when the catalysis is carried out in the presence of trolox or MPG would indicate generation of free O_2^- by the catalyst. Indeed, addition of these reductants to a film of the Cu-free catalyst resulted in higher ring currents, the magnitude of the increase correlating with the relative rate constants for O_2^- reduction by the scavengers used. In contrast, no statistically meaningful effect was observed in analogous experiments with the FeCu catalyst. It was concluded that the distal Cu ion prevents O_2^- releasing autoxidation of oxygenated catalyst via an unknown mechanism.[125] Faster degradation of oxygenated Cu-free complex was also observed in noncatalytic experiments under nonprotic conditions. If such an effect is present in mitochondria, it would decrease the flux of O_2^- from 3 to 4% to the actually observed value: 1−2% of the consumed O_2.[146]

The effect of the distal Cu ion on the susceptibility of biomimetic catalysts **19** to inhibition by CN^- and CO was also studied.[156] The cytotoxicity of CN^- is due to formation of a stable oxidized CcO−CN adduct, whose reduction by ferrocytochrome *c* is unfavorable, resulting in respiratory shutdown.[158] Because humans have an active CN^- detoxification pathway,[158] tolerance to CN^- is determined in large part by the kinetic and thermodynamic affinity of oxidized CcO to CN^-. The relative affinities of biomimetic complexes **19** to CN^-, N_3^-, and CO were comparable to those reported for CcO, although the absolute affinities were lower for the oxidized and higher for the reduced catalysts. This was attributed to the more efficient stabilization of charged species in the more polar environment experienced by the catalysts in contact with aqueous electrolyte relative to the protein matrix around the heme/Cu site in CcO. The authors compared[156] the catalytic properties of **19**FeCu and the Cu-free analogues for O_2 reduction in the presence of CN^- at pH 7 and non-turnover-limiting electron flux (to eliminate any effect of Cu on the catalytic reactivity per se). The amount of CN^- that causes a 2-fold decrease in the catalytic activity of **19a**FeCu at physiologically relevant potentials is up to 5 times higher than that of the Cu-free analogue. The higher tolerance of **19a**FeCu catalyst toward CN^- was due to the 20 mV more positive $Fe^{III/II}$ potentials and the 2.5 lower affinity of both the oxidized $Fe^{III}Cu^{II}$ and reduced $Fe^{II}Cu^{I}$ forms. The latter was unexpected, because the affinity does not appear to correlate with the overall positive charge on the complex (which is higher for **19a**FeCu than for **19a**Fe).[156] While both electrochemical and spectroscopic evidence suggests that Cu^I and Cu^{II} bind CN^- as a fourth ligand, calculations suggest that such binding would not introduce enough steric congestion in the heme pocket to significantly affect the affinity of Fe. Qualitatively similar results were observed with CO, but the difference in susceptibilities of the FeCu and Cu-free derivatives of **19** was only about 2-fold. These results contrast with findings that Cu-less cytochrome bo oxidase from *Escherichia coli* binds CN^-, N_3^-, F^-, and formate with significantly lower affinities than does the wild type.[157] Conceivably, charge compensation, which is relatively more important in the low-polarity protein environment around the heme/Cu site, obscures more subtle steric or electronic effects that disfavor CN^- or N_3^- binding to **19**Fe/Cu in direct contact with an aqueous electrolyte.

4. Conclusions

A great deal of creative effort has been expended in designing, synthesizing, and studying functional models of heme enzymes involved in O_2 transport, storage, and utilization. Such work has provided a significant body of new information relevant to understanding the chemistry of, and the structure/reactivity relationship within, the binding pockets of Mb and Hb and at the catalytic site of heme/Cu terminal oxidases.

Biomimetic studies of Mb and Hb have clearly identified the minimum stereoelectronic requirements for reversible oxygenation of ferroheme, at least in nonprotic environments. Important initial experiments have demonstrated that embedding ferroheme in a sufficiently large hydrophobic envelope allows reversible O_2 binding, even in protic media. This work is in large part motivated by the desire to

develop "blood substitutes".[159,160] A synthetic Fe porphyrin with an *M* value in a certain range can now be rationally designed on the basis of the paradigm that steric strain localized directly over the Fe atom decreases CO binding more strongly than that of O_2. A more polar binding pocket appears to enhance the effect of sterics in CO vs O_2 discrimination. However, utilization of polarity alone has not yet produced Fe porphyrins with biologically relevant *M* values. It has been speculated in reference to Mb and Hb that "it is easier to place H-bond donors at strategic positions in the protein that it is to engineer a protein scaffold near the iron atom that is rigid enough to exploit small geometry difference between the bound ligands." [25] The reverse has so far been true in biomimetic chemistry. As biomimetic chemists, we would remain skeptical of the "polarity" hypothesis in Mb until a polar mechanism of discrimination is at least reproduced outside the protein matrix, much less can be used to rationally design O_2 carriers.

The biomimetic studies of cytochrome *c* oxidase have concentrated on understanding the role of Cu_B in O_2 reduction. Electrochemistry constitutes the only technique developed so far to study the catalytic properties of synthetic heme/Cu analogues under steady-state turnover and physiologically relevant conditions of pH, electrochemical potential, and electron flux. It has been shown that the distal Cu is obligatory for O_2 reduction activity under biologically relevant turnover-determining electron flux.[155] In contrast, when electrons are in excess, distal Cu has a limited effect on the mechanism and kinetics of O_2 reduction at steady state or the stability of the catalyst.[125] On the basis of these observations, it was hypothesized that, during O_2 reduction by CcO, Cu_B may serve largely as an electron storage ("preloading") site that does not, however, provide an O_2 reduction pathway with activation energy significantly lower than that available for the heme alone exposed to excess of electrons. On the basis of these data, it was speculated that Cu_B is essential to achieve rapid 4e reduction of O_2 using electrons from slowly diffusing ferrocytochrome *c*.

In closing, we cannot help but to point out directions in biomimetic studies of hemoproteins involved in O_2 transport, storage, and reduction that, in our opinion, are most promising with respect to understanding not only the biochemical issues, but also the fundamental problem of transition-metal catalyzed activation of small molecules.

The design of biomimetic analogues of ever-closer structural similarity to the active sites of Mb, Hb, and CcO is the requirement for continuing progress in the area. In the Mb and Hb arena, design of superstructures with biologically relevant H-bond donors is critical to probe the effect of polarity on O_2 and CO binding kinetics and thermodynamics. Novel solutions for obtaining reversible O_2 binding in protic media are necessary. No developments in synthetic models of Hb cooperativity have been made in the past 15 years. It can be expected, however, that an increasing interest in "molecular machines" and means of molecular control will stimulate attempts to realize biologically relevant allosteric mechanisms in synthetic molecular and supramolecular systems.

In the arena of CcO's heme/Cu analogues, of note is the absence of studies with bimetallic complexes mimicking the histidyl−tyrosine linkage (Figure 10). Inclusion of such a redox-active, protic group will certainly add complexity to the chemical behavior of these Fe/Cu models. Development of methodologies to better mimic the conditions of steady-state O_2 reduction at the heme/Cu site of CcO is probably the most interesting and most challenging area of biomimetic studies of the enzyme. An ambitious but potentially very promising solution lies in incorporating biomimetic catalysts into self-assembled monolayers (SAMs) on electrodes. This would provide a better-defined chemical environment relative to that accessible in current methods based on films of undefined morphology at the electrode surface. In addition, it would allow control over the rate of electron transfer from the electrode to the catalytic site, thereby mimicking temporal control of electron delivery to the heme/Cu site as a result of diffusional reaction between cytochrome oxidase and ferrocytochrome *c* in vivo. However, novel cytochrome oxidase model compounds functionalized for incorporation into SAMs are required. Finally, a true functional analogue of the heme/Cu oxidases must act as a proton pump. Since the process is based on spatial separation of protons, mimicking it requires well-defined three-dimensional assemblies on the nano- or microscale. Due to the challenges in creating such assemblies and a poorly understood molecular basis for directional movement of protons against an electrochemical gradient, modeling the proton pumping capacity of cytochrome oxidase with a synthetic system is probably a longer-term target.

5. Acknowledgments

J.P.C. thanks all co-workers who appear as coauthors in cited references for their invaluable contributions to biomimetic studies of Mb, Hb, and cytochrome *c* oxidase in his laboratories. Long-standing financial support from the NIH and NSF for this biomimetic work in the J.P.C. labs is gratefully acknowledged.

6. Supporting Information Available

Tabulated data used to create Figure 6. This material is available free of charge via the Internet at http://www.pubs.acs.org.

7. References

(1) Alberts, B.; Johnson, A.; Lewis, J.; Raff, M.; Walter, P. *Molecular Biology of the Cell*; Garland Science: New York, 2002.
(2) Moodie, A. D.; Ingledew, W. J. *Adv. Microb. Physiol.* **1990**, *31*, 225.
(3) Gunsalus, R. P. In *Encyclopedia of Microbiology*, 2nd ed.; Lederberg, J., Ed.; Academic Press: San Diego, 2000; Vol. 1.
(4) Coates, J. D.; Mechaelidou, U.; Bruce, R. A.; O'Connor, S. M.; Crespi, J. N.; Achenbach, L. A. *Appl. Environ. Microbiol.* **1999**, *65*, 5234.
(5) Barrientos, A.; Barros, M. H.; Valnot, I.; Rotig, A.; Rustin, P.; Tzagoloff, A. *Gene* **2002**, *286*, 53.
(6) Kitagawa, T. *J. Inorg. Biochem.* **2000**, *82*, 9.
(7) Yoshikawa, S.; Shinzawa-Itoh, K.; Tsukihara, T. *J. Inorg. Biochem.* **2000**, *82*, 1.

(8) Wikstrom, M. *Biochim. Biophys. Acta* **2000**, *1458*, 188.
(9) Mills, D. A.; Florens, L.; Hiser, C.; Qian, J.; Ferguson-Miller, S. *Biochim. Biophys. Acta* **2000**, *1458*, 180.
(10) Babcock, G. T. *Proc. Natl. Acad. Sci. U.S.A.* **1999**, *96*, 12971.
(11) Michel, H.; Behr, J.; Harrenga, A.; Kannt, A. *Annu. Rev. Biophys. Biomol. Struct.* **1998**, *27*, 329.
(12) (a) Michel, H. *Biochemistry* **1999**, *38*, 15129. (b) Michel, H. *Nature* **1999**, *402*, 602.
(13) Babcock, G. T.; Wikstrom, M. *Nature* **1992**, *356*, 301.
(14) Pereira, M. M.; Santana, M.; Teixeira, M. *Biochim. Biophys. Acta* **2001**, *1505*, 185 and references therein.
(15) Riggs, A. F. *Curr. Opin. Struct. Biol.* **1991**, *1*, 915.
(16) *Disorders of Hemoglobin: Genetics, Pathophysiology, and Clinical Management*; Steinberg, M. H., Forget, B. G., Higgs, D. R., Nagel, R. L., Eds.; Cambridge University Press: Cambridge, 2001.
(17) Eaton, W. A.; Henry, E. R.; Hofrichter, J.; Mozzarelli, A. *Nat. Struct. Biol.* **1999**, *6*, 351.
(18) Perutz, M. F. In *Molecular Basis of Blood Diseases*; Stamatoyannopoulos, G., Ed.; Saunders: Philadelphia, 1987.
(19) Flogel, U.; Merx, M. W.; Godecke, A.; Decking, U. K. M.; Schrader, J. *Proc. Natl. Acad. Sci. U.S.A.* **2001**, *98*, 735.
(20) Moller, J. K. S.; Skibsted, L. H. *Chem. Rev.* **2002**, *102*, 1167.
(21) Springer, B. A.; Sligar, S. G.; Olson, J. S.; Phillips, G. N., Jr. *Chem. Rev.* **1994**, *94*, 699.
(22) Momenteau, M.; Reed, C. A. *Chem. Rev.* **1994**, *94*, 659.
(23) Spiro, T. G.; Zgierski, M. Z.; Kozlowski, P. M. *Coord. Chem. Rev.* **2001**, *219*, 923.
(24) Slebodnick, C.; Ibers, J. A. *JBIC, J. Biol. Inorg. Chem.* **1997**, *2*, 521.
(25) Spiro, T. G.; Kozlowski, P. M. *Acc. Chem. Res.* **2001**, *34*, 137 and references therein.
(26) Shikama, K. *Chem. Rev.* **1998**, *98*, 1357.
(27) Lomatsu, T.; Hayakawa, S.; Tsuchida, E.; Nishide, H. *Chem. Commun.* **2003**, 50.
(28) Komatsu, T.; Moritake, M.; Nakagawa, A.; Tsuchida, E. *Chem. Eur. J.* **2002**, *8*, 5469.
(29) Tsuchida, E.; Komatsu, T.; Arai, K.; Yamada, K.; Nishide, H.; Fuhrhop, J. *Langmuir* **1995**, *11*, 1877 and references therein.
(30) Jiang, D.; Aida, T. *Chem. Commun.* **1996**, 1523.
(31) Trent, J. T.; Hargrove, M. S. *J. Biol. Chem.* **2002**, *277*, 19538.
(32) Burmester, T.; Weich, B.; Reinhardt, S.; Hankein, T. *Nature* **2000**, *407*, 520.
(33) Zaslavsky, D.; Gennis, R. B. *Biochim. Biophys. Acta* **2000**, *1458*, 164.
(34) Rogers, M. S.; Dooley, D. M. *Adv. Protein Chem.* **2001**, *58*, 387.
(35) Tsukihara, T.; Aoyama, H.; Yamashita, E.; Tomizaki, T.; Yamaguchi, H.; ShinzawaItoh, K.; Nakashima, R.; Yaono, R.; Yoshikawa, S. *Science* **1996**, *272*, 1136.
(36) Iwata, S.; Ostermeier, C.; Ludwig, B.; Michel, H. *Nature* **1995**, *376*, 660.
(37) Collman, J. P.; Boulatov, R.; Sunderland, C. J. In *The Porphyrin Handbook*; Kadish, K. M., Smith, K. M., Guilard, R., Eds.; Academic Press: Boston, 2003; Vol. 11, p 1.
(38) Collman, J. P.; Wagenknecht, P. S.; Hutchison, J. E. *Angew. Chem.* **1994**, *106*, 1620.
(39) Junemann, S. *Biochim. Biophys. Acta* **1997**, *1321*, 107.
(40) Kim, E.; Chufan, E. E.; Kamaraj, K.; Karlin, K. D. *Chem. Rev.* **2004**, *104*, 1077 (in this issue).
(41) Raven, E. L.; Mauk, A. G. *Adv. Inorg. Chem.* **2001**, *51*, 1.
(42) (a) Ozaki, S. i.; Matsui, T.; Roach, M. P.; Watanabe, Y. *Coord. Chem. Rev.* **2000**, *198*, 39. (b) Lombardi, A.; Nastri, F.; Pavone, V. *Chem. Rev.* **2001**, *101*, 3162.
(43) Sigman, J. A.; Kim, H. K.; Zhao, X.; Carey, J. R.; Lu, Y. *Proc. Natl. Acad. Sci.* **2003**, *100*, 3629.
(44) Collman, J. P.; Fu, L. *Acc. Chem. Res.* **1999**, *32*, 455.
(45) Naruta, Y.; Sasaki, T.; Tani, F.; Tachi, Y.; Kawato, N.; Nakamura, N. *J. Inorg. Biochem.* **2001**, *83*, 239.
(46) Kendrew, J. C.; Bodo, G.; Dintzis, H. M.; Parrish, R. G.; Wyckoff, H. W.; Phillips, D. C. *Nature* **1958**, *181*, 662.
(47) Kendrew, J. C.; Dickerson, R. E.; Strandberg, B. E.; Hart, R. G.; Davies, D. R.; Phillips, D. C.; Shore, V. C. *Nature* **1960**, *185*, 422.
(48) Perutz, M. F.; Rossmann, M. G.; Cullis, A. F.; Muirhead, H.; Will, G.; North, A. C. T. *Nature* **1960**, *185*, 416.
(49) Cullis, A. F.; Muirhead, H.; Perutz, M. F.; Rossmann, M. G.; North, A. C. T. *Proc. R. Soc. A* **1962**, *265*, 161.
(50) Ostermann, A.; Tanaka, I.; Engler, N.; Niimura, N.; Parak, F. G. *Biophys. Chem.* **2002**, *95*, 183.
(51) Vojtechovsky, J.; Chu, K.; Berendzen, J.; Sweet, R. M.; Schlichting, I. *Biophys. J.* **1999**, *77*, 2153.
(52) Tame, J. R. H.; Vallone, B. *Acta Crystallogr.* **2000**, *D56*, 805.
(53) Shaanan, B. *Nature* **1982**, *296*, 682.
(54) Imai, K. *Allosteric Effects in Haemoglobin*; Cambridge University Press: Cambridge, 1982.
(55) Pauling, L.; Weiss, J. J. *Nature* **1964**, *203*, 182.
(56) Kitagawa, T.; Ohfrias, M. R.; Rousseau, D. L.; Ikeda-Saito, M.; Yonetani, T. *Nature* **1982**, *298*, 869.
(57) Phillips, S. E. V. *Mol. Biol.* **1980**, *142*, 531.
(58) Phillips, S. E. V.; Schoenborn, B. P. *Nature* **1981**, *292*, 81.
(59) Goldberg, D. E. *Chem. Rev.* **1999**, *99*, 3371.
(60) Metz, G.; Sjostrand, T. *Acta Physiol. Scand.* **1954**, *31*, 334.
(61) Wang, J. H.; Nakahara, A.; Fleischer, E. E. *J. Am. Chem. Soc.* **1958**, *80*, 1109.
(62) Balasubramanian, S.; Lambright, D. G.; Simmons, J. H.; Gill, S. J.; Boxer, S. G. *Biochemistry* **1994**, *33*, 8355.
(63) Sigfridsson, E.; Ryde, U. *J. Biol. Inorg. Chem.* **1999**, *4*, 99 and references therein.
(64) Jameson, G. B. In *Metal-Containing Polymeric Materials*; Carraher, C., Zeldin, M., Sheats, J., Culbertson, B., Pittman, C. U., Jr., Eds.; Plenum: New York, 1996.
(65) Huang, X.; Boxer, S. G. *Nat. Struct. Biol.* **1994**, *1*, 226.
(66) Collman, J. P.; Herrmann, P. C.; Fu, L.; Eberspacher, T. A.; Eubanks, M.; Boitrel, B.; Hayoz, P.; Zhang, X. M.; Brauman, J. I.; Day, V. W. *J. Am. Chem. Soc.* **1997**, *119*, 3481.
(67) Collman, J. P.; Broring, M.; Fu, L.; Rapta, M.; Schwenninger, R.; Straumanis, A. *J. Org. Chem.* **1998**, *63*, 8082.
(68) Tang, H.; Dolphin, D. *Inorg. Chem.* **1996**, *35*, 6539.
(69) Johnson, M. R.; Seok, W. K.; Ma, W. P.; Slebodnick, C.; Wilcoxen, K. M.; Ibers, J. A. *J. Org. Chem.* **1996**, *61*, 3298.
(70) Slebodnick, C.; Fettinger, J. C.; Peterson, H. B.; Ibers, J. A. *J. Am. Chem. Soc.* **1996**, *118*, 3216.
(71) Tani, F.; Matsu-ura, M.; Ariyama, K.; Setoyama, T.; Shimada, T.; Kobayashi, S.; Hayashi, T.; Matsuo, T.; Hisaeda, Y.; Naruta, Y. *Chem. Eur. J.* **2003**, *9*, 865.
(72) Collman, J. P.; Brauman, J. I.; Iverson, B. L.; Sessler, J. L.; Morris, R. M.; Gibson, Q. H. *J. Am. Chem. Soc.* **1983**, *105*, 3052.
(73) Collman, J. P.; Brauman, J. I.; Doxsee, K. M.; Sessler, J. L.; Morris, R. M.; Gibson, Q. H. *Inorg. Chem.* **1983**, *22*, 1427.
(74) Tsuchida, E.; Komatsu, T.; Kumamoto, S.; Ando, K.; Nishide, H. *J. Chem. Soc., Perkin Trans. 2* **1995**, 747.
(75) Komatsu, T.; Sano, K.; Tsuchida, E. *Chem. Commun.* **1998**, 977.
(76) Tsuchida, E.; Komatsu, T.; Arai, K.; Nishide, H. *J. Chem. Soc., Dalton Trans.* **1993**, 2465.
(77) Komatsu, T.; Okada, T.; Moritake, M.; Tsuchida, E. *Bull. Chem. Soc. Jpn.* **2001**, *74*, 1695.
(78) (a) Momenteau, M.; Loock, B.; Lavalette, D.; Tetreau, C.; Mispelter, J. *J. Chem. Soc., Chem. Commun.* **1983**, 962. (b) Gerothannasis, I. P.; Momenteau, M.; Loock, B. *J. Am. Chem. Soc.* **1989**, *111*, 7006.
(79) El-Kasmi, D.; Tetreau, C.; Lavalette, D.; Momenteau, M. *J. Am. Chem. Soc.* **1995**, *117*, 6041.
(80) Tetreau, C.; Lavalette, D.; Momenteau, M.; Fischer, J.; Weiss, R. *J. Am. Chem. Soc.* **1994**, *116*, 11840.
(81) Traylor, T. G.; Koga, N.; Deardurff, L. A. *J. Am. Chem. Soc.* **1985**, *107*, 6504.
(82) David, S.; James, B. R.; Dolphin, D.; Traylor, T. G.; Lopez, M. A. *J. Am. Chem. Soc.* **1994**, *116*, 6.
(83) Zingg, A.; Felber, B.; Gramlich, V.; Fu, L.; Collman, J. P.; Diederich, F. *Helv. Chim. Acta* **2002**, *85*, 333.
(84) Collman, J. P.; Sunderland, C. J.; Boulatov, R. *Inorg. Chem.* **2002**, *41*, 2282.
(85) Tsuchida, E.; Komatsu, T.; Yanagimoto, T. *J. Porphyrins Phthalocyanines* **2000**, *4*, 81.
(86) Weyermann, P.; Diederich, F. *J. Chem. Soc., Perkin Trans.* **2000**, 4231.
(87) Collman, J. P.; Brauman, J. I.; Halbert, T. R.; Suslick, K. S. *Proc. Natl. Acad. Sci. U.S.A.* **1976**, *73*, 3333.
(88) Tetreau, C.; Leondiadis, L.; Lavalette, D.; Momenteau, M. *J. Chem. Soc., Perkin Trans.* **1992**, 73.
(89) Ray, G. B.; Li, X. Y.; Ibers, J. A.; Sessler, J. L.; Spiro, T. G. *J. Am. Chem. Soc.* **1994**, *116*, 162.
(90) Momenteau, M.; Scheidt, W. R.; Eigenbrot, C. W.; Reed, C. A. *J. Am. Chem. Soc.* **1988**, *110*, 1207.
(91) Jameson, G. B.; Ibers, J. A. *J. Am. Chem. Soc.* **1980**, *102*, 2823.
(92) Kim, K.; Ibers, J. A. *J. Am. Chem. Soc.* **1991**, *113*, 6077.
(93) Kim, K.; Fettinger, J.; Sessler, J. L.; Cyr, M.; Hugdahl, J.; Collman, J. P.; Ibers, J. A. *J. Am. Chem. Soc.* **1989**, *111*, 403.
(94) Collman, J. P.; Schwenninger, R.; Rapta, M.; Broring, M.; Fu, L. *Chem. Commun.* **1999**, 137.
(95) Wuenschell, G. E.; Tetreau, C.; Lavalette, D.; Reed, C. A. *J. Am. Chem. Soc.* **1992**, *114*, 3346.
(96) Collman, J. P.; Zhang, X. M.; Wong, K.; Brauman, J. I. *J. Am. Chem. Soc.* **1994**, *116*, 6245.
(97) Chang, C. K.; Liang, Y.; Aviles, G. *J. Am. Chem. Soc.* **1995**, *117*, 4191.
(98) Collman, J. P.; Berg, K. E.; Sunderland, C. J.; Aukauloo, A.; Vance, M. A.; Solomon, E. I. *Inorg. Chem.* **2002**, *16*, 6583.
(99) Collman, J. P.; Sunderland, C. J.; Berg, K. E.; Vance, M. A.; Solomon, E. I. *J. Am. Chem. Soc.* **2003**, *125*, 6648.
(100) Tsuchida, E.; Nishide, H.; Yuasa, M.; Sekine, M. *Chem. Lett.* **1983**, 473.
(101) See for example: Shinkai, S.; Ikeda, M.; Sugasaki, A.; Takeuchi, M. *Acc. Chem. Res.* **2001**, *34*, 494.
(102) Tsuchida, E.; Hasegawa, E.; Honda, K. *Biochim. Biophys. Acta* **1976**, *427*, 520.
(103) Collman, J. P.; Brauman, J. I.; Rose, E.; Suslick, K. S. *Proc. Natl. Acad. Sci. U.S.A.* **1978**, *75*, 1052.

(104) Jameson, G. B.; Molinaro, F. S.; Ibers, J. A.; Collman, J. P.; Brauman, J. I.; Rose, E.; Suslick, K. S. *J. Am. Chem. Soc.* **1980**, *102*, 3224.
(105) Bayer, E.; Holzbach, G. *Angew. Chem., Int. Ed. Engl.* **1977**, *16*, 117.
(106) Tabushi, I.; Sasaki, T. *J. Am. Chem. Soc.* **1983**, *105*, 2901.
(107) Tabushi, I.; Kugimiya, S.; Sasaki, T. *J. Am. Chem. Soc.* **1985**, *107*, 5159.
(108) Tabushi, I.; Kugimiya, S. *J. Am. Chem. Soc.* **1986**, *108*, 6926.
(109) Abramson, J.; Svensson-Ek, M.; Byrne, B.; Iwata, S. *Biochim. Biophys. Acta* **2001**, *1544*, 1.
(110) Abramson, J.; Riistama, S.; Larsson, G.; Jasaitis, A.; Svensson-Ek, M.; Laakkonen, L.; Puustinen, A.; Iwata, S.; Wikstrom, M. *Nat. Struct. Biol.* **2000**, *7*, 910.
(111) (a) Pinakoulaki, E.; Pfitzner, U.; Ludwig, B.; Constantinos, V. C. *J. Biol. Chem.* **2002**, *277*, 13563. (b) Proshlyakov, D. A.; Pressler, M. A.; DeMaso, C.; Leykam, J. F.; DeWitt, D. L.; Babcock, G. T. *Science* **2000**, *290*, 1588.
(112) Morgan, J. E.; Verkhovsky, M. I.; Palmer, G.; Wikstroem, M. *Biochemistry* **2001**, *40*, 6882.
(113) Mogi, T.; Hirano, T.; Nakamura, H.; Anraku, Y.; Orii, Y. *FEBS Lett.* **1995**, *370*, 259.
(114) Brown, S.; Rumbley, J. N.; Moody, A. J.; Thomas, J. W.; Gennis, R. B.; Rich, P. R. *Biochim. Biophys. Acta* **1994**, *1183*, 521.
(115) Calhoun, M. W.; Hill, J. J.; Lemieux, L. J.; Ingledew, W. J.; Alben, J. O.; Gennis, R. B. *Biochemistry* **1993**, *32*, 11524.
(116) Lemon, D. D.; Calhoun, M. W.; Gennis, R. B.; Woodruff, W. H. *Biochemistry* **1993**, *32*, 11953.
(117) Hosler, J. P.; Ferguson-Miller, S.; Calhoun, M. W.; Thomas, J. W.; Hill, J.; Lemieus, L.; Ma, J.; Georgiou, C.; Fetter, J.; Shapleigh, J. P. *J. Bioenerg. Biomembr.* **1993**, *25*, 121.
(118) Hunter, D. J. B.; Moody, A. J.; Rich, P. R.; Ingledew, W. J. *FEBS Lett.* **1997**, *412*, 43.
(119) Shapleigh, J. P.; Hosler, J. P.; Tecklenburg, M. M. J.; Kim, Y.; Babcock, G. T.; Gennis, R. B.; Ferguson-Miller, S. *Proc. Natl. Acad. Sci. U.S.A.* **1992**, *89*, 4786.
(120) (a) Blomberg, M. R. A.; Siegbahn, P. E. M.; Babcock, G. T.; Wikstrom, M. *J. Am. Chem. Soc.* **2000**, *122*, 12848. (b) Blomberg, M. R. A.; Siegbahn, P. E. M.; Wikstrom, M. *Inorg. Chem.* **2003**, *42*, 5231.
(121) Klibanov, A. M. *Nature* **2001**, *409*, 241.
(122) *Enzymatic Reactions in Organic Media*; Koskinen, A. M., Klibanov, A. M., Eds.; Blackie-Pergamon: London, 1996.
(123) Weitzman, P. D. J.; Watkins, P. J. In *Enzyme Assays: A Practical Approach*; Eisenthal, R., Danson, M. J., Eds.; Oxford University Press: Oxford, 1992.
(124) Bard, A. J.; Faulkner, L. R. *Electrochemical Methods*; Wiley: New York, 2001.
(125) Boulatov, R.; Collman, J. P.; Shiryaeva, I. M.; Sunderland, C. J. *J. Am. Chem. Soc.* **2002**, *124*, 11923.
(126) (a) Collman, J. P.; Rapta, M.; Broring, M.; Raptova, L.; Schwenninger, R.; Boitrel, B.; Fu, L.; L'Her, M. *J. Am. Chem. Soc.* **1999**, *121*, 1387. (b) Collman, J. P.; Fu, L.; Herrmann, P. C.; Zhang, X. M. *Science* **1997**, *275*, 949.
(127) Collman, J. P.; Broring, M.; Fu, L.; Rapta, M.; Schwenninger, R. *J. Org. Chem.* **1998**, *63*, 8084.
(128) (a) Ricard, D.; L'Her, M.; Richard, P.; Boitrel, B. *Chem. Eur. J.* **2001**, *7*, 3291. (b) Didier, A.; L'Her, M.; Boitrel, B. *Org. Biomol. Chem.* **2003**, *1*, 1274.
(129) Verkhovsky, M. I.; Morhan, J. E.; Wikstrom, M. *Biochemistry* **1995**, *34*, 7483.
(130) Rich, P. R.; Moody, A. J. In *Bioenergetics*; Graber, P., Milazzo, G., Eds.; Birkhauser: Basel, 1997; Vol. 4.
(131) The $Fe^{III/II}$ potential of the synthetic heme/Cu analogues in Figure 14 is ~0.15 V (vs NHE);[37] for heme, this potential is ~ −0.1 V under comparable experimental conditions (Pilloud, D. L.; Chen, X.; Dutton, P. L.; Moser, C. C. *J. Phys. Chem. B* **2000**, *104*, 2868).
(132) Likewise, knowledge of the electrochemical behavior of Cu centers alone under conditions similar to those at which electrocatalysis is observed is equally important for gaining a complete understanding of the electrocatalytic properties of heme/Cu analogues. Unfortunately, little is known about O_2 reactivity of Cu^I or of Cu^I complexes in aqueous media under electrochemical conditions. Simple Cu^I salts generate H_2O_2 and subsequently hydroxyl radicals via Fenton chemistry (see for example: Tomat, R.; Salmaso, R.; Zecchin, S. *Electrochim. Acta* **1994**, *39*, 2475). A porphyrinatozinc derivative, **19**ZnCu, is not electrocatalytically active when adsorbed on a graphite electrode at pH 7,[125] which is not unexpected as **19**ZnCu^I is aerobically stable. However, electron transfer in films of **19**ZnCu appears to be significantly retarded, which may affect the observed chemistry. There is some indication that **21**ZnCu behaves similarly.[126] Little else is known on this subject.
(133) Shiryaeva, I. M.; Collman, J. P.; Boulatov, R.; Sunderland, C. J. *Anal. Chem.* **2003**, *79*, 494.
(134) Collman, J. P.; Fudickar, W.; Shiryaeva, I. M. *Inorg. Chem.* **2003**, *42*, 3384.
(135) Kobayashi, N.; Nishiyama, Y. *J. Electroanal. Chem.* **1984**, *181*, 107.
(136) Shi, C.; Anson, F. C. *Inorg. Chem.* **1990**, *29*, 4298.
(137) Shigehara, K.; Anson, F. C. *J. Phys. Chem.* **1982**, *86*, 2776.
(138) Oyaizu, K.; Haryono, A.; Natori, J.; Shinoda, H.; Tsuchida, E. *Bull. Chem. Soc. Jpn.* **2000**, *73*, 1153.
(139) Forshey, P. A.; Kuwana, T. *Inorg. Chem.* **1983**, *22*, 699.
(140) Su, Y. O.; Kuwana, T.; Chen, S. M. *J. Electroanal. Chem.* **1990**, *288*, 177.
(141) Bettelheim, A.; Parash, R.; Ozer, D. *J. Electrochem. Soc.* **1982**, *129*, 2247.
(142) Kobayashi, N.; Osa, T. *J. Electroanal. Chem.* **1983**, *157*, 269.
(143) Sono, M.; Roach, M. P.; Coulter, E. D.; Dawson, J. H. *Chem. Rev.* **1996**, *96*, 2841.
(144) Kalish, H. R.; Latos-Grazynski, L.; Balch, A. L. *J. Am. Chem. Soc.* **2000**, *122*, 12478.
(145) Cunningham, I. D.; Danks, T. N.; O'Connel, K. T. A.; Scott, P. W. *J. Chem. Soc., Perkin Trans. 2* **1999**, 2133.
(146) Huie, R. E.; Neta, P. In *Reactive Oxygen Species in Biological Systems*; Gilbert, D. L., Colton, C. A., Eds.; Kluwer: New York, 1999.
(147) Cabelli, D. E. In *Peroxyl Radicals*; Alfassi, Z. B., Ed.; Wiley: New York, 1997.
(148) *Active Oxygen in Chemistry*; Foote, C. S., Valentine, J. S., Greenberg, A., Liebman, J. E., Eds.; Chapman: New York, 1995.
(149) Collman, J. P.; Shiryaeva, I. M.; Boulatov, R. *Inorg. Chem.* **2003**, *42*, 4807.
(150) Loetzbeyer, T.; Schuhmann, W.; Schmidt, H.-L. *J. Electroanal. Chem.* **1995**, *395*, 339.
(151) Ricard, D.; Andrioletti, B.; Boitrel, B.; L'Her, M. *Chem. Commun.* **1999**, 1523.
(152) Ricard, D.; Didier, A.; L'Her, M.; Boitrel, B. *ChemBioChem* **2001**, *2*, 144.
(153) Collman, J. P.; Fu, L.; Herrmann, P. C.; Wang, Z.; Rapta, M.; Broring, M.; Schwenninger, R.; Boitrel, B. *Angew. Chem., Int. Ed.* **1998**, *37*, 3397.
(154) Collman, J. P.; Fu, L.; Herrmann, P. C.; Zhang, X. M. *Science* **1997**, *275*, 949.
(155) Collman, J. P.; Boulatov, R. *Angew. Chem., Int. Ed.* **2002**, *41*, 3487.
(156) Collman, J. P.; Boulatov, R.; Shiryaeva, I. M.; Sunderland, C. J. *Angew. Chem., Int. Ed.* **2002**, *41*, 4139.
(157) Moody, A. J.; Mitchell, R.; Jeal, A. E.; Rich, P. R. *Biochem. J.* **1997**, *324*, 743.
(158) *Clinical and Experimental Toxicology of Cyanides*; Ballantyne, B., Marrs, T. C., Eds.; Wright: Bristol, UK, 1987.
(159) Squires, J. E. *Science* **2002**, *295*, 1002.
(160) Riess, J. G. *Chem. Rev.* **2001**, *101*, 2797.

CR0206059